HHS Public Access

Author manuscript

Cell Rep. Author manuscript; available in PMC 2024 January 28.

Published in final edited form as:

Cell Rep. 2023 November 28; 42(11): 113323. doi:10.1016/j.celrep.2023.113323.

Kruppel-like factor 2+ CD4 T cells avert microbiota-induced intestinal inflammation

Tzu-Yu Shao[1], **Tony T. Jiang**[1], **Joseph Stevens**[2], **Abigail E. Russi**[3], **Ty D. Troutman**[4], **Anas Bernieh**[5], **Giang Pham**[1], **John J. Erickson**[2], **Emily M. Eshleman**[6], **Theresa Alenghat**[6], **Stephen C. Jameson**[7], **Kristin A. Hogquist**[7], **Casey T. Weaver**[8], **David B. Haslam**[1], **Hitesh Deshmukh**[2], **Sing Sing Way**[1,9,*]

[1]Division of Infectious Diseases, Center for Inflammation and Tolerance, University of Cincinnati School of Medicine, Cincinnati, OH 45229, USA

[2]Division of Neonatology and Pulmonary Biology, University of Cincinnati School of Medicine, Cincinnati, OH 45229, USA

[3]Division of Gastroenterology, Hepatology and Advanced Nutrition, University of Cincinnati School of Medicine, Cincinnati, OH 45229, USA

[4]Division of Allergy and Immunology, University of Cincinnati School of Medicine, Cincinnati, OH 45229, USA

[5]Division of Pathology, University of Cincinnati School of Medicine, Cincinnati, OH 45229, USA

[6]Division of Immunobiology, Cincinnati Children's Hospital Medical Center, University of Cincinnati School of Medicine, Cincinnati, OH 45229, USA

[7]Center for Immunology, Department of Laboratory Medicine and Pathology, University of Minnesota Medical School, Minneapolis, MN 55455, USA

[8]Program in Immunology, University of Alabama at Birmingham Heersink School of Medicine, Birmingham, AL 35233, USA

[9]Lead contact

SUMMARY

Intestinal colonization by antigenically foreign microbes necessitates expanded peripheral immune tolerance. Here we show commensal microbiota prime expansion of CD4 T cells unified by the Kruppel-like factor 2 (KLF2) transcriptional regulator and an essential role for KLF2+ CD4 cells

*Correspondence: singsing.way@cchmc.org.

AUTHOR CONTRIBUTIONS

Conceptualization, T.-Y.S., T.T.J., J.S., A.E.R., T.D.T., S.C.J., K.A.H., H.D., and S.W.; funding acquisition, S.S.W.; investigation, T.-Y.S., T.T.J., J.S., A.E.R., T.D.T., T.A., D.B.H., H.D., and S.S.W.; methodology, T.-Y.S., T.T.J., J.S., A.E.R., A.B., G.P., J.J.E., E.M.E., T.A., S.C.J., K.A.H., C.T.W., D.B.H., and H.D.; project administration, T.-Y.S. and S.S.W.; supervision, S.S.W.; writing – original draft, T.-Y.S., A.E.R., and S.S.W.; writing – review & editing, all authors.

DECLARATION OF INTERESTS

The authors declare no competing interests.

SUPPLEMENTAL INFORMATION

Supplemental information can be found online at https://doi.org/10.1016/j.celrep.2023.113323.

in averting microbiota-driven intestinal inflammation. CD4 cells with commensal specificity in secondary lymphoid organs and intestinal tissues are enriched for KLF2 expression, and distinct from FOXP3+ regulatory T cells or other differentiation lineages. Mice with conditional KLF2 deficiency in T cells develop spontaneous rectal prolapse and intestinal inflammation, phenotypes overturned by eliminating microbiota or reconstituting with donor KLF2+ cells. Activated KLF2+ cells selectively produce IL-10, and eliminating IL-10 overrides their suppressive function *in vitro* and protection against intestinal inflammation *in vivo*. Together with reduced KLF2+ CD4 cell accumulation in Crohn's disease, a necessity for the KLF2+ subpopulation of T regulatory type 1 (Tr1) cells in sustaining commensal tolerance is demonstrated.

In brief

Intestinal colonization by antigenically foreign microbes necessitates expanded immune tolerance. Shao et al. show commensal microbiota prime expansion of immune suppressive IL-10-producing CD4 T cells identified by the transcriptional regulator Kruppel-like factor 2 (KLF2), and the necessity for KLF2+ CD4 cells in averting microbiota-driven intestinal inflammation.

Graphical Abstract

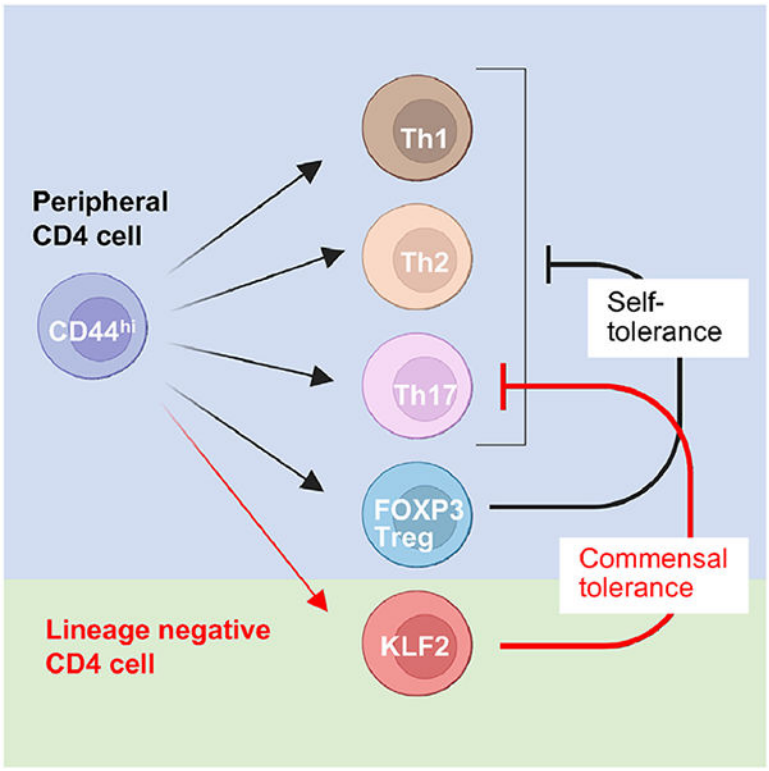

INTRODUCTION

The intestine and other mucosal barrier tissues harbor trillions of microbes that are antigenically foreign. Unavoidable contact with commensal microbiota highlights the need for expanded peripheral immune tolerance. Our current framework for investigating how

tolerance expands in this context is primarily focused on the immune-suppressive FOXP3+ subset of CD4 cells called regulatory T cells (Tregs).[1–6] This Treg-centric focus stems from classical observations that intestinal inflammation occurs with multi-organ systemic autoimmunity in humans and mice with naturally occurring FOXP3 deficiency,[7–10] or when FOXP3+ cells are depleted throughout the lifespan.[11] A variety of commensal microbe species or their metabolites also selectively prime CD4 cell differentiation into FOXP3+ Tregs.[12–17] Although these results clearly show FOXP3+ cell involvement, their necessity for averting microbiota-induced intestinal inflammation remains uncertain.

An important caveat is intestinal inflammation that still occurs after depletion of FOXP3+ cells for mice housed under germ-free gnotobiotic conditions, with comparable expansion of pro-inflammatory Th17 CD4 cells.[18] These findings highlight unresolved questions as to why eliminating the microbiota does not more dramatically bypass the need for Tregs in mucosal tissues. One consideration is that FOXP3+ Tregs are equally essential for restraining activation of T cells with microbe *and* self-reactivity, so eliminating the microbiota alone does not override the need for FOXP3+ cells in maintaining self-tolerance in barrier tissue such as the intestine. An alternative explanation is that FOXP3+ Treg suppression of autoimmunity in mucosal tissues masks the importance of other cells with more focused roles in sustaining commensal tolerance. Non-overlapping roles between FOXP3+ and other cells that protect against microbiota-driven intestinal inflammation could explain the curious observation that inflamed tissues in human inflammatory bowel disease consistently show non-reduced, and often increased FOXP3+ Tregs.[19–21] A necessity for FOXP3-negative cells for maintaining microbiota tolerance may also reconcile why some commensal microbes, such as segmented filamentous bacteria or *Candida albicans* (Ca), establish intestinal colonization at high densities, including mono-colonization, without pathological inflammation despite limited priming of microbe-specific FOXP3+ Tregs.[22–24] With these considerations, approaches for more in-depth analysis of T cells with commensal specificity were developed, with particular attention to strategies capable of uncoupling FOXP3+ Tregs from cells with potentially more focused roles in maintaining commensal tolerance.

RESULTS

Commensal stimulation primes lineage-negative KLF2+ CD4 T cells

To track CD4 cells with commensal microbiota specificity, recombinant Ca engineered to constitutively express a recombinant protein containing the I-A^b-restricted $2W1S_{55–68}$ peptide (Ca-2W1S) was used to establish intestinal colonization for mice in our specific pathogen-free facility naturally devoid of commensal fungi.[24–26] Endogenous CD4 cells with I-A^b:$2W1S_{55–68}$ surrogate fungal specificity were analyzed given their elevated precursor frequency for mice on the C57BL/6 background.[27] We showed high-density (>10^6 CFU per gram tissue), long-term (>60 days) Ca-2W1S colonization throughout the small and large intestine without clinical symptoms is achieved by drinking water with ampicillin supplementation, which mimics antibiotic-induced human Ca colonization.[24,28] Intestinal Ca-2W1S colonization primes ~30-fold expansion of I-A^b:$2W1S_{55–68}$ CD4 cells with surrogate commensal specificity in secondary lymphoid organs (spleen plus peripheral

lymph nodes), which are nearly all CD44^{hi}, reflecting antigen-induced activation[24,29] (Figure 1A). Staining for lineage-defining markers shows that commensal Ca-2W1S-primed CD4 cells differentiate into RORγt+ Th17 cells (26%), PD1+ CXCR5+ BCL6+ Tfh cells (10%), IRF4+ Th2 cells (7%), with ≤5% FOXP3+ Tregs, or TBET+ Th1 cells (Figures 1A and S1A). Interestingly, this distribution does not account for nearly half the expanded pool of CD44^{hi} cells with commensal specificity in Ca2W1S-colonized mice compared with >90% Th1 differentiation for cells of the same specificity primed in other contexts including intestinal *Salmonella typhimurium* or parenteral *Listeria monocytogenes* infection[30,31] (Figure S1B).

To further investigate the commensal Ca-2W1S-primed response, sort purified I-A^{b}:2W1S+ CD44^{hi} CD4 cells were evaluated using single-cell gene expression profiling, which confirmed accumulation of cells with Th17 and Tfh profiles with substantially reduced Th2 and Tregs, and no Th1 cells (Figure 1B). This analysis also verified that nearly half the commensal Ca-2W1S-primed cells did not cluster into established differentiation lineages, and were instead unified by Kruppel-like factor 2 (KLF2) expression (Figure 1B), a zinc finger transcriptional regulator previously shown to control T cell thymic egress, trafficking to secondary lymphoid organs, and repressed Tfh differentiation.[32–34] Comparatively, few cells in Th17, Th2, Treg, or Tfh clusters expressed KLF2 (Figure 1C), with distinct gene expression profiles for cells in each differentiation cluster compared with lineage-negative KLF2+ cells (Figure S2; Table S1). I-A^{b}:2W1S lineage-negative cells in Ca-2W1S-colonized mice also did not show increased expression of anergic T cell makers FR4 and CD73 (Figure S1C), highlighting distinctions between cells of the same specificity primed by peptide feeding that models food antigen stimulation.[35]

KLF2 expression was further evaluated after Ca-2W1S colonization in KLF2(GFP) reporter mice[34] given the lack of available anti-KLF2 antibodies that work with flow cytometry. These experiments verified that ~30% I-A^{b}:2W1S cells with commensal Ca-2W1S specificity were KLF2(GFP)+, and significantly increased compared with tetramer-negative CD44^{hi} CD4 cells with irrelevant bulk specificity (Figure 1D). Importantly, enriched KLF2 expression was not limited only to cells with commensal fungal specificity, since similarly increased KLF2+ cells were found among mesenteric lymph node (mLN) and intestinal CD4 cells with I-A^{b}:CBir1$_{464–472}$ specificity to bacterial flagellin compared with tetramer-negative CD44^{hi} cells with irrelevant bulk specificity[36–38] (Figures 1E and S3). Tonic commensal stimulation sustains accumulation of KLF2+ CD4 cells with commensal specificity since levels of KLF2+ CBir1+ cells numerically contract in the mLN and each intestinal tissue after drinking water supplementation with an antibiotic cocktail (ampicillin, gentamicin, metronidazole, neomycin, vancomycin) that eliminates commensal bacteria[26,39,40] (Figure 1E). Thus, stimulation by a variety of intestinal commensal microbes primes expanded accumulation of KLF2+ CD4 cells.

Spontaneous colitis in mice lacking KLF2+ CD4 T cells

The *in vivo* necessity for KLF2+ cells was evaluated using mice with conditional loss of KLF2 in T cells, generated by intercrossing CD4^{Cre} with KLF2 floxed (KLF2$^{f/f}$) transgenic strains.[41,42] Interestingly, spontaneous rectal prolapse with colonic shortening developed

in over half the CD4^{Cre} KLF2$^{f/f}$ mice by age ~100 days compared with co-housed Cre-negative KLF2$^{f/f}$ littermate controls (Figures 2A and S4). These phenotypes paralleled increased granulocyte and plasma cell infiltration in the colonic lamina propria and crypt elongation (Figure 2B), elevated fecal levels of several pro-inflammatory cytokines including GCSF, IL-17A, IL-1α, IL-1β, along with the highly sensitive inflammation marker, Lipocalin2[43] (Figures 2C and 2D). In turn, mLN levels of RORγt+ Th17 effectors and FOXP3+ Tregs were each significantly elevated in CD4^{Cre} KLF2$^{f/f}$ mice compared with Cre-negative littermate controls (Figure 2E). Microbiota are essential since these clinical and immunological indicators of intestinal inflammation were each overturned after drinking water supplementation with the aforementioned five-antibiotic cocktail that eliminates commensal bacteria (Figure 2). Thus, KLF2 expression in T cells protects against microbiota-driven intestinal inflammation.

Increased mLN accumulation of FOXP3+ cells in colitogenic CD4^{Cre} KLF2$^{f/f}$ mice was especially interesting given the reported role of KLF2 for Treg differentiation and migration to secondary lymphoid organs.[44,45] We considered if commensal tolerance is primarily attributed to FOXP3+ Tregs, why expanded mLN accumulation of these cells in CD4^{Cre} KLF2$^{f/f}$ mice does not protect against intestinal inflammation. The possibility that Treg suppressive function requires cell-intrinsic KLF2 expression and intestinal inflammation in mice with KLF2-deficient T cells reflects FOXP3+ cells with diminished suppressive function was evaluated by comparing Tregs from CD4^{Cre} KLF2$^{f/f}$ or WT mice using established *in vitro* suppression assays.[46,47] Tregs in CD4^{Cre} KLF2$^{f/f}$ mice were purified based on GITR and CD25 co-expression, which showed high (≥94%) sensitivity and specificity despite the expected shifts in Helios, Neuropilin (Nrp1), CD44, and CD62L expression[44,45] (Figures 3A and 3B). Interestingly, these experiments showed that purified GITR+ CD25+ mLN CD4 cells in CD4^{Cre} KLF2$^{f/f}$ mice have enhanced (non-reduced) suppressive function (Figure 3C), indicating that KLF2 is not only non-essential, but may restrain suppression in FOXP3+ cells. Thus, microbiota-dependent intestinal inflammation in CD4^{Cre} KLF2$^{f/f}$ mice, which occurs despite expanded accumulation of functionally suppressive FOXP3+ cells, further highlights potential non-overlapping roles between Tregs and FOXP3-negative KLF2+ cells, with the latter essential for protecting against microbiota-driven intestinal inflammation.

KLF2 identifies immune-suppressive activated CD4 cells

Suppressive properties linked with KLF2 were directly evaluated using sort purified cells from KLF2(GFP) reporter mice, which showed dose-dependent suppressive function for KLF2(GFP)+ CD44^{hi} CD4 cells (Figure 4A), similar to that described for Tregs.[46,47] Importantly, suppression by KLF2(GFP)+ cells was uncoupled from FOXP3+ cells, since purified KLF2(GFP)+ CD44^{hi} FOXP3(RFP)-negative cells from KLF2(GFP) FOXP3(RFP) dual reporter mice retained suppressive function, and with potency similar to FOXP3(RFP)+ cells (Figure 4B). Suppression by KLF2(GFP)+ CD44^{hi} cells was also not explained by their potential differentiation into Tregs, since FOXP3 expression remained at background levels compared with retained FOXP3 expression by the majority of FOXP3(RFP)+ cells after responder cell co-culture (Figure 4C).

Suppressive function among FOXP3(RFP)-negative cells was limited to KLF2(GFP) + CD44^{hi} cells, with ~8-fold increased potency compared with KLF2(GFP)-negative CD44^{hi} or KLF2(GFP)+ CD44^{lo} cells, which did not significantly impact responder cell proliferation (Figure 4D). Differences in suppressive function were also not explained by discordant proliferation since Ki67 levels were uniformly increased for each FOXP3(RFP)-negative subset regardless of suppressive potency (Figure S5). The role of KLF2 in FOXP3+ cells was further evaluated by comparing suppressive potency of FOXP3(RFP)+ Tregs subdivided exclusively based on KLF2 expression, since Tregs did not contain a defined population of KLF2+ CD44^{hi} cells (Figure 4D). These experiments showed modestly reduced (~2-fold) suppressive potency for KLF2(GFP)+ compared with KLF2(GFP)-negative FOXP3(RFP)+ cells, which is in sharp contrast to enhanced suppressive function by activated KLF2+ FOXP3-negative cells (Figure 4D). Together with enhanced suppressive potency of GITR+ CD25+ (FOXP3)+ mLN cells from CD4^{Cre} KLF2$^{f/f}$ mice (Figure 3B), these results suggest KLF2 plays opposing roles, impeding suppression in FOXP3+ cells while promoting suppression in FOXP3-negative CD44^{hi} cells.

To further investigate the importance of KLF2+ CD4 cell suppression *in vivo*, these cells were evaluated using an established model of intestinal inflammation involving transfer of CD45RB^{hi} cells to lymphopenic recipients.[48–50] These experiments showed significantly reduced fecal Lipocalin2 levels in *Rag1−/−* mice co-transferred KLF2(GFP) + CD44^{hi} FOXP3(RFP)-negative with CD45RB^{hi} cells compared with mice transferred CD45RB^{hi} cells alone (Figure 4E). Likewise, proliferation measured by BrdU incorporation among mLN CD45RB^{hi} CD4 cells (distinguished from KLF2+ CD4 cells based on CD45.1 congenic marker expression) was reduced in mice co-transferred KLF2(GFP)+ with CD45RB^{hi} cells compared with mice transferred only CD45RB^{hi} cells (Figure 4F). As with *in vitro* suppression, protection against these intestinal inflammation parameters by co-transferred KLF2(GFP)+ FOXP3(RFP)-negative was comparable with co-transferred FOXP3(RFP)+ cells (Figures 4E and 4F), and not explained by differentiation into classical Tregs since FOXP3 expression remained at background levels (Figure 4G). Thus, suppression by KLF2+ cells is dissociated from FOXP3+ Tregs, with comparable *in vitro* and *in vivo* suppressive properties for each cell type.

KLF2+ CD4 cells mediate suppression via IL-10

To determine how KLF2+ CD4 cells mediate suppression, initial experiments evaluated whether they share with FOXP3+ Tregs the necessity for cell-intrinsic TCR stimulation.[46] These studies show that polyclonal KLF2+ CD44^{hi} FOXP3(RFP)-negative cells do not suppress proliferation of monoclonal CD4 cells from BG2 TCR transgenic mice in response b-gal cognate peptide stimulation[51] (Figure 5A), which is in sharp contrast to suppressed responder cell proliferation when both KLF2+ CD44^{hi} and responder cells receive TCR stimulation (Figure 4A). Given these requirements for TCR cell-intrinsic stimulation, gene expression distinctions between KLF2+ CD44^{hi} compared with KLF2-negative CD44^{hi} cells were evaluated before and after TCR stimulation. This analysis showed that *Gzma, Il10*, and *Ube2c* expression were most increased among stimulated KLF2+ CD44^{hi} cells (Figure 5B; Table S2). IL-10 was particularly interesting given the susceptibility of *Il10*−/− mice to commensal microbiota-driven intestinal inflammation,[52–54] and the importance of IL-10

produced by FOXP3-negative CD4 T regulatory type 1 (Tr1) cells for averting intestinal inflammation.[55,56] Complementary experiments verified that IL-10 protein production occurs selectively by purified KLF2+ CD44^{hi} cells upon TCR stimulation compared with background levels by KLF2-negative cells (Figure 5C); and, more importantly, that suppression by purified KLF2+ CD44^{hi} cells is overturned by anti-IL-10- or anti-IL-10 receptor-neutralizing antibodies (Figure 5D).

Although IL-10-producing FOXP3-negative cells have been described in a wide variety of contexts, and loosely classified together as Tr1 cells,[56–58] unifying features including the transcription factor(s) controlling their differentiation and IL-10 production remain uncertain. To further investigate the interplay between IL-10, KLF2, and FOXP3, cells producing IL-10 were evaluated using 10BiT IL-10(CD90.1) reporter mice[55] intercrossed with KLF2(GFP); FOXP3(RFP) mice. When gated on FOXP3(RFP)-negative cells, we found that IL-10 production is restricted to CD44^{hi} cells, and increased among KLF2+ compared with KLF2-negative cells after *in vivo* TCR stimulation (Figure 5E). IL-10-producing KLF2+ compared with KLF2-negative cells also show elevated co-expression of some, but not all classical Tr1 markers (Figures 5E and S6A). For example, expression of LAG3, CD226, CD39, and CTLA4 were each significantly increased among IL-10-producing KLF2+ cells, whereas CD49b expression levels were similar compared with IL-10-producing KLF2-negative cells. Expanded analysis of all IL-10-producing CD4 cells (including FOXP3+ cells) across tissues showed KLF2 expression by a majority (~65%) of IL-10+ FOXP3-negative cells in the spleen and mLN. Comparatively, KLF2 positivity is sharply reduced among intestinal FOXP3-negative and FOXP3+ cells in Peyer's patch and lamina propria (Figure S6B), highlighting interesting KLF2 expression heterogeneity by IL-10-producing CD4 cells across tissues.

Besides IL-10, a variety of other molecules implicated in mediating suppression by Tr1 cells including TGF-β, CTLA4, and ICOS[55,59–62] are also expressed more by KLF2+ upon anti-TCR stimulation (Table S2). However, *in vitro* neutralization of these and other molecules associated with Tr1 suppression, individually or in combination with IL-10 receptor blockade, does not further override suppression by KLF2+ CD44^{hi} cells beyond IL-10 receptor blockade (Figure 5D). Thus, a majority of IL-10-producing FOXP3-negative CD4 cells in secondary lymphoid organs (spleen and mLN) are identified by KLF2, which co-express several classical Tr1-defining markers. However, 40%–70% of IL-10-producing CD4 cells in intestinal tissues express neither KLF2 nor FOXP3, further underscoring heterogeneity of IL-10-producing CD4 cells beyond these transcriptional regulators.

To more definitively investigate the cellular source of IL-10 required for averting intestinal inflammation, how intestinal inflammation in CD4^{Cre} KLF2$^{f/f}$ mice is impacted by adoptively transferred KLF2+ CD44^{hi} donor cells from WT compared with *Il10*−/− mice was evaluated. These experiments demonstrating reduced fecal Lipocalin2 and mLN accumulation of RORγt+ IL-17A-producing cells in mice reconstituted with WT donor KLF2+ CD44^{hi} cells (Figures 5F and 5G) further highlight that intestinal inflammation in CD4^{Cre} KLF2$^{f/f}$ mice is caused by the absence of activated KLF2+ cells. In turn, this platform also establishes the importance of IL-10 production by KLF2+ cells since neither reductions in fecal Lipocalin2 levels nor mLN accumulation of IL-17A-producing Th17

cells were found in $CD4^{Cre}$ $KLF2^{f/f}$-recipient mice reconstituted with KLF2+ $CD44^{hi}$ cells from *Il10*−/− donors (Figures 5F and 5G). Taken together, these results show that activated KLF2+ cells selectively produce IL-10, and that IL-10 production by KLF2+ $CD44^{hi}$ cells is essential for averting commensal microbiota-driven intestinal inflammation.

Uncoupling intestinal inflammation from peripheral lymphopenia

Since KLF2 controls expression of sphingosine-1-phosphate receptor 1 (S1PR1) and CD62L required for T cell thymic egress and lymphoid organ homing, mice with KLF2-deficient T cells have dramatically reduced T cells in the blood, spleen, and secondary lymphoid organs with normal levels in non-lymphoid tissues.[33,34] To uncouple intestinal inflammation from peripheral lymphopenia in $CD4^{Cre}$ $KLF2^{f/f}$ mice, we compared the impacts of induced KLF2 deletion (tamoxifen administration to $CD4^{CreER(T2)}$ $KLF2^{f/f}$ mice) with administration of the S1PR1 modulator FTY720.[63,64] Despite slightly more accelerated tempo of peripheral CD4 cell decline and loss of CD62L expression in FTY720-treated compared with tamoxifen-treated $CD4^{CreER(T2)}$ $KLF2^{f/f}$ mice (Figure 6A), intestinal inflammation shown by increasing fecal Lipocalin2 levels and mLN accumulation of RORγt+ Th17 cells was only observed in mice with conditional KLF2 deficiency (Figures 6B and 6C). Importantly, these intestinal inflammation phenotypes occurring after induced KLF2 deletion are microbiota driven, since eliminating intestinal bacteria using the aforementioned five-antibiotic cocktail normalizes each parameter (fecal Lipocalin2 levels, mLN RORγt+ Th17 cell accumulation, and histological inflammation) (Figures 6B–6D). Further analysis of commensal-specific cells, with either $I\text{-}A^b$:2W1S commensal fungi specificity in tamoxifen-treated Ca-2W1S colonized $CD4^{CreER(T2)}$ $KLF2^{f/f}$ mice or cells with $I\text{-}A^b$:CBir1 bacterial flagellin specificity in tamoxifen-treated SPF mice, show similarly increased RORγt+ Th17 mLN CD4 cells after induced KLF2 deletion compared with cells in Cre-negative littermate controls (Figure 6E). Thus, KLF2+ CD4 cells are not only essential for averting microbiota-driven inflammation but actively sustain commensal tolerance, since induced loss of these cells causes intestinal inflammation associated with reciprocally expanded Th17 effector CD4 cells with commensal specificity.

Reduced KLF2+ CD4 T cells in Crohn’s disease

Crohn’s disease is a chronic disorder associated with intestinal inflammation. While the underlying pathogenesis remains undefined, clear causative associations exist with intestinal dysbiosis and microbiota-driven inflammation; and defects in suppressing inflammation in each context.[65–67] To investigate potential KLF2+ CD4 T cell defects, publicly available single-cell gene expression datasets from three separate studies[68–70] containing biopsy specimensfrom20individualswithCrohn’sdisease and 8controlswere evaluated together. Broad consideration of all CD4 cells, including Tfhand Treg cells, in each dataset using previously described clustering approaches[68] (Figure S7), showed significantly reduced KLF2+ CD4 cells in Crohn’s disease inflamed tissue compared with controls (Figure 7A; Table S3). In agreement with predominant KLF2 expression by lineage-negative murine CD4 cells (Figure 1), focused analysis on Treg or Tfh clusters showed sharply reduced KLF2+ cells (Figure 7B). Comparatively, FOXP3+ cells in Crohn’s disease were not significantly different among total CD4 cells or individual subsets (Figures 7A and 7B).

Thus, inflamed tissue in Crohn's disease is associated with reduced KLF2+ CD4 T cells, and particularly among non-Tfh and non-Treg CD4 T cells.

Gene expression analyses highlight additional KLF2+ CD4 cell distinctions in Crohn's disease. For example, KLF2+ CD4 T cells from Crohn's disease compared with controls show reduced expression of the KLF2-induced chemokine receptorCCR7[45] (Figure 7C; Table S4). Cells from individuals with Crohn's disease also have reduced expression of glucocorticoid-induced leucine zipper, known to suppress intestinal inflammation when overexpressed in CD4 cells,[71] and the zinc-finger RNA binding protein ZFP36C2, which inhibits lymphocyte proliferation[72] (Figure 7C; Table S4). In turn, the cAMP-responsive element modulator that promotes production of IL-17A and other pro-inflammatory cytokines,[73] and IRF1 known to control Th17 and Th1 cell activation,[74] were each expressed to higher levels by KLF2+ CD4 T cells from individuals with Crohn's disease (Figure 7C). Complementary gene ontology analysis of all differentially expressed genes shows that KLF2+ CD4 T cells in controls compared with Crohn's disease are more highly enriched in pathways associated with MHC class II antigen processing and presentation, along with Treg differentiation, neutrophil chemotaxis, and T cell co-stimulation (Figure S9). Comparatively, KLF2+ CD4 T cells in Crohn's disease were more highly enriched in pathways associated with regulation of acute inflammation, stress response, and lipoprotein remodeling (Figure S9). Thus, the necessity for KLF2+ CD4 T cells in averting commensal microbiota-driven intestinal inflammation in mice is recapitulated by naturally reduced accumulation of these cells in human Crohn's disease. Besides, for numerical reductions, remaining KLF2+ CD4 cells in Crohn's disease have distinct gene expression and ontogeny profiles that likely further promote the immune pathogenesis of inflammatory bowel disease.

DISCUSSION

Commensal microbes have co-evolved with mammalian hosts to promote a variety of increasingly recognized physiological benefits.[5,75,76] Microbe sensing requires expanded immune tolerance to protect against aberrant inflammation. Our findings demonstrate that KLF2+ CD4 cells are essential for this physiological imperative. Colonization selectively primes KLF2+ cells with commensal specificity (Figure 1), and intestinal inflammation spontaneously develops in mice with constitutive or induced KLF2 deficiency in CD4 cells (Figures 2 and 6). These protective roles are dissociated from FOXP3+ Tregs given expansion of FOXP3+ cells that retain suppressive function in colitogenic mice without KLF2+ cells (Figure 3), and similar suppressive potency among purified KLF2+ FOXP3-negative compared with FOXP3+ cells *in vitro* and *in vivo*, occurring without FOXP3 acquisition (Figure 4). Interestingly, while KLF2 identifies $CD44^{hi}$ FOXP3-negative cells with suppressive function, KLF2 expression in FOXP3+ cells plays non-contributory or opposing effects impeding suppressive function, shown by reduced suppressive potency of KLF2+ compared with KLF2-negative FOXP3+ cells (Figure 4D), and increased suppressive potency of GITR+ CD25+ Tregs from $CD4^{Cre}$ $KLF2^{f/f}$ compared with control mice (Figure 3C). Variable penetrance of autoimmunity phenotypes including cachexia, inflamed ears, oily skin, and hair loss for $FOXP3^{Cre}$ $KLF2^{f/f}$ mice with conditional loss of KLF2 in FOXP3+ cells,[45] suggests that enhanced suppressive potency does not bypass the importance of KLF2-dependent tissue homing for FOXP3+ Tregs. However, we find

only a small proportion of antigen-experienced KLF2+ CD4 cells co-express FOXP3, or fall into Treg gene expression clusters (Figures 1, 4, and 7). In turn, inflamed tissue in human Crohn's disease is associated with diminished KLF2+ CD4 cell accumulation, with reductions magnified among non-Treg, non-Tfh clusters (Figure 7). These considerations, together with non-reduced FOXP3+ Tregs in inflamed Crohn's disease tissue,[19–21] suggest non-overlapping functional roles between KLF2+ and FOXP3+ cells in protecting against microbiota-driven intestinal inflammation.

Identification of microbiota-stimulated CD4 cells with suppressive function, distinct from FOXP3+ Tregs, and their necessity for averting microbiota-induced intestinal inflammation reconciles several inconsistencies exclusively ascribing commensal tolerance to FOXP3+ cells. This includes intestinal inflammation that persists after FOXP3+ cell depletion in germ-free mice,[18] which indicates the importance of classical Tregs in sustaining self-tolerance, whereas KLF2+ cells appear to play more focused roles protecting against microbiota-driven inflammation given the efficiency whereby eradicating commensal bacteria overrides intestinal inflammation for mice with constitutive or induced KLF2 deficiency (Figures 2 and 6). KLF2 expression was demonstrated for a large proportion of systemic and intestinal CD4 cells with specificity to recombinant Ca-2W1S and bacterial flagellin CBir1 commensal antigens (Figure 1), establishing a framework for why intestinal inflammation does not occur despite high-density mono-colonization with other microbes such as segmented filamentous bacteria that do not prime FOXP3+ Treg expansion.[22,23] Thus, while some microbial species selectively promote FOXP3+ Treg differentiation,[12–17] commensal microbe-replete mice containing Tregs with these specificities still do not bypass the necessity for KLF2+ CD4 cells in averting intestinal inflammation.

FOXP3-negative KLF2+ cells selectively produce IL-10, and IL-10 is essential for their suppressive function shown *in vitro* using classical assays with responder cell co-culture and *in vivo* given the inability of *Il10*−/− donor KLF2+ cells to override intestinal inflammation in recipient mice with KLF2-deficient T cells. IL-10 utilization in this context dovetails nicely with the unambiguous protective role this cytokine plays in averting intestinal inflammation[52] and microbiota-induced colitis in *Il10*−/− mice.[53,54] Although IL-10-producing CD4 cells have been extensively characterized in a variety of contexts, with FOXP3-negative cells uniformly lumped together as Tr1 cells,[56–58] there remains no consensus on unifying markers including Tr1 lineage-defining transcriptional regulators and/or suppressive molecules beyond IL-10. We propose that this reflects phenotypic and functional heterogeneity among FOXP3-negative IL-10-producing CD4 cells, which is further highlighted by differences in KLF2 expression. For example, while IL-10 production is enriched among FOXP3-negative KLF2+ CD44^{hi} splenocytes, ~20% that express neither FOXP3 nor KLF2 cells still produce IL-10 after anti-TCR *in vivo* stimulation (Figure 5E). Likewise, while a majority (~65%) of IL-10-producing FOXP3-negative cells in the spleen and mLN co-express KLF2 (Figure S6B), KLF2 positivity is sharply reduced among IL-10-producing intestinal (Peyer's patch plus small and large intestine lamina propria) CD4 cells, further underscoring heterogeneity between Tr1 cells within and across tissues. FOXP3-negative IL-10-producing KLF2+ CD44^{hi} cells also show increased expression of some (LAG3, CD226, CD39, CTLA4), but not all markers (CD49b) used for identifying Tr1 cells,[56–58] whereas molecules such as TGF-β and CTLA4 shown to mediate suppression by

Tr1 cells in other contexts appear to play non-contributory roles for KLF2+ cells (Figure 5D).[55,59–62] With this heterogeneity in mind, our data identify KLF2 as a non-exclusive marker for Tr1 cells; but, more importantly, the IL-10-producing subset of FOXP3-negative CD4 cells most essential for averting commensal microbiota-driven intestinal inflammation. Appreciating heterogeneity among FOXP3-negative IL-10-producing cells may reconcile ongoing inconsistencies for how Tr1 cells are currently identified, and promote further investigation on how IL-10 produced by more narrowly defined FOXP3-negative CD4 cell subpopulations work in other defined physiological contexts.

Heterogeneity in IL-10-producing FOXP3-negative cells also opens up additional questions for how distinct CD4 subsets mediate specialized function using the same suppressive cytokine. Our data identifying an essential role for KLF2+ cells in sustaining commensal tolerance that protects against intestinal inflammation highlight another molecular distinction for further dissociating IL-10-producing CD4 cells beyond FOXP3.[77] Important next-steps include investigating how KLF2 controls IL-10 expression, and KLF2+ cells in other physiological contexts that require IL-10 (e.g., reproductive tolerance, antimicrobial host defense).[78–80] A related priority involves evaluating lineage commitment stability of commensal primed KLF2+ CD4 cells, potential history of prior FOXP3 expression by suppressive FOXP3-negative KLF2+ cells,[81] and whether KLF2+ cells can differentiate into pro-inflammatory effector lineages, and the commensal priming conditions that stimulate KLF2 and IL-10 co-expression in antigen-experienced CD4 cells. Nonetheless, an instructive alternative framework for investigating intestinal inflammation from a non-FOXP3+ Treg-centric perspective is unveiled through identification of KLF2 as a distinct suppressive CD4 subset required for averting commensal microbiota-induced inflammation in mice, and blunted accumulation of these cells in human Crohn's disease.

Limitations of the study

We recognize that whether KLF2+ and FOXP3+ cells are functionally redundant in protecting against intestinal inflammation appears to differ depending on the experimental context. For example, colitis occurs in $CD4^{Cre}$ $KLF2^{f/f}$ mice despite increased accumulation of FOXP3+ Tregs, which retain enhanced suppressive potency (Figures 2 and 3), suggesting that KLF2+ and FOXP3+ cells are functionally non-redundant for averting intestinal inflammation. However, with colitis induced in *Rag1*−/− mice by adoptively transferred $CD45RB^{hi}$ cells, co-transferred KLF2+ $CD44^{hi}$ (FOXP3-negative) or FOXP3+ cells each protects against intestinal inflammation, and purified KLF2+ cell do so without induced FOXP3 expression (Figures 4E–4G), highlighting potential functional redundancy between KLF2+ and FOXP3+ cells in this context. Resolving these differences will require further analysis using alternative preclinical models and/or analysis of human cells from individuals with intestinal inflammation. For the latter, publicly available single-cell data from intestinal biopsy specimens from three independent studies together containing 20 individuals with Crohn's disease and 8 controls when combined and evaluated together show ~50% reduced KLF2+ CD4 cells but similar Treg levels in Crohn's disease. Prior to combining data across studies, each dataset was initially re-analyzed using the same standardized clustering approach and evaluated for nonsignificant differences within each group (Crohn's disease or controls). We recognize that combining data from separate studies is not

ideal, especially since each study contained different numbers of individuals with Crohn's disease and controls, with one study containing only Crohn's disease samples. However, non-statistically significant differences considering data from each study in isolation or any pairing combination of two studies were difficult to interpret given the lack of statistical power and, for transparency, we have depicted data from each study separately using non-overlapping data symbol colors (Figure 7) or individual plots (Figures S7 and S8). Accordingly, important next steps will be to re-evaluate KLF2+ compared with FOXP3+ cells, in both intestinal biopsy specimens and the peripheral blood, in larger cohorts of individuals with inflammatory bowel disease.

STAR★METHODS

RESOURCE AVAILABILITY

Lead contact—Further information and requests for resources and reagents should be directed to and will be fulfilled by the lead contact, Dr. Sing Sing Way (singsing.way@cchmc.org).

Materials availability—Reagents describe in this paper are available from the lead contact upon request with a completed Material Transfer Agreement.

Data and code availability

- All data reported in this paper will be shared by the lead contact upon request.
- Mouse single cell and bulk RNA sequencing data have been deposited to Geo under singsingway@orcid under accession number GSE236151, and all original code has been deposited at https://github.com/Deshmukh-Lab/KLF2_WayLab. DOIs are listed in the key resources table.
- Any additional information required to reanalyze the data reported in this paper is available from the lead contact upon request.

EXPERIMENTAL MODEL AND STUDY PARTICIPANT DETAILS

Mice—Commercially available C57BL/6, CD45.1 (002014), CD90.1 (000406), $FOXP3^{RFP}$ (008374),[85] *Rag1*−/− (002216), *Il10*−/− (002251), $CD4^{Cre}$ (017336) and $CD4^{CreER(T2)}$ (022356)[86] each on the C57BL/6 background were purchased from The Jackson Laboratory, intercrossed and maintained for at least 5 generations at Cincinnati Children's Hospital. $KLF2^{GFP}$, $KLF2^{f/f}$, and 10BiT mice have been described,[34,42,55] and were intercrossed with $FOXP3^{RFP}$, *Il10*−/−, $CD4^{Cre}$ or $CD4^{CreER(T2)}$ mice. BG2 TCR transgenic mice were provided by Dr. Dale S. Gregerson.[51] All mice were housed under specific pathogen-free conditions, and experiments performed using sex- and age-matched controls under Cincinnati Children's Hospital IACUC approved protocols.

METHOD DETAILS

Microbial colonization and infection—The recombinant *C. albicans*-2W1S strain, and it's use in intestinal colonization of mice maintained on drinking water supplemented with ampicillin (1 mg/mL) has been described.[24,25] Recombinant *Listeria monocytogenes*

and *Salmonella typhimurium* (ΔAroA BMM51) each engineered to stably express the I-A^b:2W1$S_{55–68}$ peptide as a recombinant protein has each been described.[30,31] For infection, 10^9 CFU S *typhimurium* in early log-phase growth was orally administered using a 20G gavage needle, and 10^4 CFU *L monocytogenes* was intravenously inoculated via the lateral tail vein.

Cell isolation, staining and flow cytometry—Fluorophore-conjugated antibodies used for cell analysis include anti-CD4 (clone GK1.5), anti-CD8a (clone 53–6.7), anti-CD11b (clone M1/70), anti-CD11c (clone N418), anti-F4/80 (clone BM8), anti-B220 (clone RA3–6B2), anti-CD44 (clone IM7), anti-CD45 (clone 30F11), anti-CD45.1 (clone A20), anti-CD45.2 (clone 104), anti-CD90.1 (clone OX-7), anti-CD90.2 (clone 30-H12), anti-CD49b (clone DX5), anti-LAG3 (clone C9B7W), anti-CD226 (clone 10E5), anti-CD39 (clone 24DMS1), anti-CTLA4 (clone UC10–4B9), anti-RORγt (clone Q31–378), anti-FOXP3 (clone FJK-16S), anti-IRF4 (clone 34E), anti-TBET (clone 4B10), anti-BCL6 (clone K112–91), anti-PD1 (clone 29F.1A12), anti-CXCR5 (clone L138D7), anti-IL17A (clone TC 11–18H10.1), anti-Helios (clone 22F6), anti-CD304 (clone 3DS304M), anti-CD62L (clone MEL-14), anti-CD25 (clone PC61), anti-GITR (clone DTA-1), anti-Ki67 (clone 16A8).

For detecting CD4 cells with I-A^b:2W1$S_{55–68}$ surrogate *C. albicans* specificity, single cell suspension from spleen and peripheral lymph nodes of colonized or no colonization control mice were incubated with phycoerythrin (PE)- or allophycocyanin (APC) conjugated I-A^b:2W1$S_{55–68}$ tetramer at 4°C for 60 min as described.[24,27] For detecting CD4 cells with I-A^b:CBir1$_{464–472}$ specificity to bacterial flagellin, cells from the spleen, peripheral or mesenteric lymph node or each intestinal segment were incubated with PE or APC conjugated I-A^b:CBir1$_{464–472}$ tetramer at room temperature for 60 min as described.[84]

Intestinal lamina propria cells were isolated by dissecting the small and large intestine, removing the Peyer's patches, and longitudinally opening each intestinal segment followed by cutting into small pieces. To remove intestinal epithelium cells, saline washed intestinal tissue were incubated with stripping buffer (PBS with 5% FBS, 1mM EDTA, 1mM DTT) at 37°C with gentle shaking (200 rpm) for 25 min with buffer replacement after 10 min. Thereafter, the intestinal tissue (cut into ~2mm fragments) were resuspended in digestion buffer (DMEM medium supplemented with 10% FBS, 0.2 mg/mL DNase I and 2.4 mg/mL Collagenase A) at 37°C with gentle shaking for 20 min, followed by tissue passage through an 18 gauge syringe and filtering through an 100 μm cell strainer, with final leukocyte isolation using a Percoll gradient (5 mL 40% and 3mL 60%) and centrifugation at 1800 rpm for 20 min as described.[84,87,88]

Intranuclear staining was performed after cell permeabilization using commercial kits (eBioscience) according to the manufacturer's instructions. For detecting bromodeoxyuridine (BrdU) incorporation, mLN cells were subjected to intracellular staining using anti-BrdU antibody and commercially available reagents (BD). Samples were acquired using an BD FACS-Canto or LSR-Fortessa cytometer and analyzed using FlowJo software (Tree Star). For cytokine production, 2×10^6 single cell suspension from each tissue was stimulated with PMA/ionomycin (eBioscience) and brefeldin A (GolgiPlug, BD Bioscience)

in 200 μL DMEM medium (supplemented with 10% fetal bovine serum, 1% L-glutamine, 10 mM HEPES, 1% penicillin-streptomycin) at 37°C with 5% CO_2 for 5 h.

***In vitro* suppression assay—**For evaluating suppressive potency, CD4 splenocytes were initially enriched by negative selection (Miltenyi) from KLF2^{GFP} reporter or KLF2^{GFP} FOXP3^{RFP} dual reporter mice, stained with anti-CD4, anti-CD8 and anti-CD44 antibodies, followed with sorting (BD FACS-Aria). For evaluating suppression by GITR+CD25^{+} cells, mLN CD4 cells were enriched from CD4^{Cre} KLF2$^{f/f}$ or Cre-negative littermate control mice, stained anti-CD4, anti-CD8, anti-GITR, and anti-CD25 antibodies, and sort purified as GITR+CD25^{+} CD4^{+} (CD8-negative) cells. Thereafter, suppression was assayed by co-culture with 10^5 CFSE-labeled (5μM for 10 min at room temperature) responder splenocytes from congenially discordant (CD45.1 or CD90.1) mice on the B6 background, or BG-2 TCR transgenic mice, and stimulation with anti-CD3 (2.5 μg/mL, clone 145–2C11, BioXcell) and anti-CD28 (1.25 μg/mL, clone 37.51, BioXcell) or β-galactosidase peptide (500nM) or with each indicated neutralizing or isotype antibody (50 μg/mL) in 200 μL DMEM medium (supplemented with 10% fetal bovine serum, 1% L-glutamine, 10 mM HEPES, 1% penicillin-streptomycin) at 37°C with 5% CO_2 for 96 h.

Adoptive *in vivo* cell transfer—For intestinal inflammation after T cell reconstitution in *Rag1*−/− mice, splenic CD4 cells from donor CD45.1 mice were initially enriched by negative selection (Miltenyi), followed by sort purification of CD45RB^{hi} cells and intraperitoneal injection into *Rag1*−/− recipients (5×10^4 cells) as described.[48–50] For co-transfer, *Rag1*−/− recipients received CD45RB^{hi} cells (5×10^4 cells) plus either sort purified KLF2(GFP)+ CD44^{hi} FOXP3(RFP) negative or FOXP3(RFP) positive cells (5×10^5) from CD45.2 donors. For evaluating the necessity of IL10 production by KLF2+ cells, splenic CD4 cells from WT or *Il10*−/− KLF2(GFP) FOXP3(RFP) donors were initially enriched by negative selection (Miltenyi), followed by sort purification as CD44^{hi} KLF2(GFP)+ FOXP3(RFP)-negative cells, and intravenous transfer into CD4^{Cre} KLF2$^{f/f}$ recipient mice (10^6 purified donor cells per mouse).

Antibiotic, BrdU, antibody, tamoxifen, and FTY720 treatment—To eliminate commensal bacteria, the drinking water was supplemented with ampicillin (0.5 mg/mL, Sigma), gentamicin (0.5 mg/mL, Sigma), neomycin (0.5 mg/mL, Sigma), metronidazole (0.5 mg/mL, Sigma), vancomycin (0.25 mg/mL, MP Biomedicals), sucralose (1 mg/mL, Sigma) as described.[26,39] For BrdU cooperation, mice were injected with BrdU (1 mg, IP) for three consecutive days prior to tissue harvest. For evaluating IL10 production using 10BiT IL10(CD90.1) KLF2(GFP) FOXP3(RFP) mice, anti-CD3 IgG (15μg clone 145–2C11) was administered to mice IP in two equal doses 48 and 4 h prior to tissue harvest as described.[58,89] For induced KLF2 deletion, CD4$^{CreER(T2)}$ KLF2$^{f/f}$ and control mice were fed irradiated chow containing tamoxifen (400 mg/kg; Envigo). For *in vivo* sphingosine-1-phosphate receptor blockade, mice were administered FTY720 (20μg, IP) daily for 20–25 consecutive days as described.[90]

Cytokine, chemokine, Lipocalin2 detection—For detecting inflammatory cytokine/chemokines in the feces, fresh fecal pellets were weighed and homogenized in sterile saline

(100 mg/mL), supernatants collected after centrifugation (15000 rpm 10 min), and analyzed using Milliplex (Millipore, Sigma) or mouse Lipocalin-2 ELISA (R&D).

Single-cell or bulk transcriptome sequencing and analysis—Single cell suspensions were obtained from the spleen and peripheral lymph nodes of mice treated colonized with Ca-2W1S for 21 days. Following tetramer staining, *C. albicans* specific (I-A^b:2W1$S_{55–68}$) CD4 cells were flow sorted and loaded onto the Fluidigm C1 chip according to manufacturer's protocol. Each cell had a targeted read depth of 1.5–2 million reads in a 75 based-paired, paired-end fashion. This experiment was performed three times, yielding 179 total cells initially. Cell lysis, reverse transcription, cDNA synthesis and amplification were processed using the SMART-Seq v4 Ultra Low RNA Kit for the Fluidigm C1 System (Takara Inc). Library preparation and tagmentation were preformed using the Nextera XT DNA Library Preparation Kit. Pooled samples were sequenced on PE75 Flow cell (HiSeq 2500; Illumina), with single lanes each containing 120–150 million reads with paired end sequencing. Mapping was performed using AltAnalyze with reference to the mm 10 genomic dataset, and log-normalized data scaled using Seurat with additional downstream analysis performed in R (version4.3.0). Filtering was performed to retain cells with more than 3000 genes and percent mitochondrial reads less than 2% in Seurat (version 4.0.2) as described.[91] Potential doublets were excluded by removing cells expressing more than 6500 genes. The post-filtration dataset contained 174 cells. Gene expression was log-normalized, and cell identities were assigned using a supervised assessment for expression of known lineage defining markers (TBX21 for Th1, IRF4 for Th2, CXCR5 for Tfh and FOXP3 for Treg), with the remaining unlabeled cells categorized as lineage-negative. The 'SeuratFindAllMarkers' function was used to identify subset specific genes (expressed by a minimum of 20% of the cells; log2 fold-change >0.5, p value <0.05). Pairwise comparisons (Figure S2) were also performed to identify subset-specific differentially expressed genes in comparison to KLF2 expressing T-helper cells using the default parameters of the 'SeuratFindMarkers'function and 'only.pos = FALSE'. These analyses were visualized as 'volcano plots' using ggplot2, with DEGs annotated by subset specific coloring (p value ≤ 0.05 & absolute value of the average log2 fold-change >0).

For comparing gene expression changes in KLF2+ cells upon stimulation, 5 million sort purified KLF2+ $CD44^{hi}$ and KLF2-negative $CD44^{hi}$ FOXP3-negative cells were stimulated with anti-CD3 (2.5 μg/mL, clone 145–2C11, BioXcell) and anti-CD28 (1.25 μg/mL, clone 37.51, BioXcell) for 48 h, with RNA isolation thereafter using RNeasy mini kit (Qiagen). RNA was subjected to cDNA synthesis and sequencing using the SMARTer Stranded Total RNA-Seq Pico Input Mammalian Kit v3 (Takara Inc). Briefly, RNA fragmentation and cDNA synthesis followed by addition of Illumina-based indexed adapters and enzymatic rRNA depletion, and a second round of PCR to generate the final sequence library. Pooled samples were then subjected to sequencing (NovaSeq 6000; Illumina) to an average of 100 million 150 nucleotide paired end reads per sample. RNAseq raw reads were subject to quality control and filtering using Sickle (version 1.33). Reads were then aligned to the mouse genome (GRCm38) using STAR default setting,[92] and counts outputted at the gene and exon level in tabular format using FeatureCounts within the R Subread package.[82] Differentially expressed gene (DEG) analysis was performed in DESeq2.[83]

For analysis of human single cell gene expression, the preprocessed and annotated scRNAseq data from previously published studies were obtained.[68–70,93] Cell type classifications from Elmentaite et al.[68] were used to annotate cells in studies by Jaeger et al.[69] and Martin et al.[70] for consistency using *TransferData* function[94] in Seurat 4.0. KLF2+ and FOXP3+ CD4 T cells were identified using *WhichCells* function in Seurat 4.0. Frequencies of either KLF2+ and FOXP3+ cells relative to total number of CD4 T cells for each subject were determined. We identified differentially expressed genes (DEG) in CD4 T cells between healthy controls and inflamed Crohn's disease samples in studies by Elmentaite et al.[68] and Jaeger et al.[69] We did not perform DEG analysis for study by Martin et al.[70] as it lacked matched samples from healthy subjects. DEG were calculated using FindMarkers in Seurat 4.0. After removing cell quality-associated markers, DEG with a fold change of ≥2 and t test p value of ≤0.05 (FDR corrected) were used for functional enrichment analysis of biological processes using PANTHER.[95] Overrepresented pathways in each disease condition were visualized with ggplot2. To construct heatmaps of DEG, genes were filtered to have a two-sided p value < 0.05 by Seurat 4.0's implementation of the Wilcoxon rank-sum test, and the average log (fold-change) of each DE gene plotted.

Histopathology—Colon tissue fixed with 10% formalin for at least 24 h before embedded in paraffin and Hematoxylin and eosin (H&E) staining of intestinal tissue was performed by the Pathology Core at Cincinnati Children's Hospital, and scored in a blinded fashion using a 10 point scale (1–5 for inflammation/lymphoid hyperplasia severity; and 1–5 for degree of crypt elongation).

QUANTIFICATION AND STATISTICAL ANALYSIS

All statistical analyses were performed with Prism (GraphPad). The two-tailed Mann-Whiney U test was used to evaluate differences between groups for non-normally distributed datasets, and the two-tailed Student's t test used for normally distributed datasets. Ordinary one-way ANOVA was used to evaluate experiments containing more than two groups. Rectal prolapse curve were analyzed by the Log rank (Mantel-Cox) test. For each analysis, $p < 0.05$ was taken as statistical significance. Iowa Russ Lenth's power and sample size calculator for independent two sample pooled t test, assuming a normal distribution and standard deviation of 0.33 of the mean, was used for human sample size calculations.

Supplementary Material

Refer to Web version on PubMed Central for supplementary material.

ACKNOWLEDGMENTS

We are indebted to the faculty in the Center for Inflammation and Tolerance for helpful discussions, Krystal Seger for technical assistance, the staff of Research Animal Resources at Cincinnati Children's Hospital led by Dr. Saigiridhar Tummala for the conscientious care of mice, and the NIH Tetramer Core Facility (supported by NIH-NIAID contract 75N93020D00005) for providing PE and APC-conjugated MHC class II I-A^b:2W1$S_{55–68}$ and I-A^b:CBir1$_{464–472}$ tetramers. All flow cytometric data were acquired using equipment maintained by the Research Flow Cytometry Facility in the Division of Rheumatology at Cincinnati Children's Hospital Medical Center, and we would like to acknowledge their assistance in sample acquisition and processing. This work was supported by NIH-NIAID through grants DP1AI131080, R01AI168222, and R01AI172960, and by NIH-NIDDK through grant P30-DK078392 Pathology Core of the Digestive Diseases Research Core at Cincinnati Children's Hospital. S.S.W. is also supported by the March of Dimes Ohio Collaborative on Prematurity Research, HHMI

Faculty Scholar's program (grant no. 55108587) and Burroughs Wellcome Fund Investigator in the Pathogenesis of Infectious Disease Award (grant no. 1011031). J.S. is supported by NHLBI training grant F30HL165594; A.E.R. is supported by NIDDK training grant T32DK007727 (PI, Denson); J.J.E. is supported by NICHD training grant K12HD028827 (PI, Cheng).

INCLUSION AND DIVERSITY

We support inclusive, diverse, and equitable conduct of research.

REFERENCES

1. Belkaid Y, and Hand TW (2014). Role of the microbiota in immunity and inflammation. Cell 157, 121–141. 10.1016/j.cell.2014.03.011. [PubMed: 24679531]
2. Maynard CL, Elson CO, Hatton RD, and Weaver CT (2012). Reciprocal interactions of the intestinal microbiota and immune system. Nature 489, 231–241. 10.1038/nature11551. [PubMed: 22972296]
3. Honda K, and Littman DR (2016). The microbiota in adaptive immune homeostasis and disease. Nature 535, 75–84. 10.1038/nature18848. [PubMed: 27383982]
4. Russler-Germain EV, Rengarajan S, and Hsieh CS (2017). Antigen-specific regulatory T-cell responses to intestinal microbiota. Mucosal Immunol. 10, 1375–1386. 10.1038/mi.2017.65. [PubMed: 28766556]
5. Hooper LV, Littman DR, and Macpherson AJ (2012). Interactions between the microbiota and the immune system. Science 336, 1268–1273. 10.1126/science.1223490. [PubMed: 22674334]
6. Tanoue T, Atarashi K, and Honda K (2016). Development and maintenance of intestinal regulatory T cells. Nat. Rev. Immunol. 16, 295–309. 10.1038/nri.2016.36. [PubMed: 27087661]
7. Hori S, Nomura T, and Sakaguchi S (2003). Control of regulatory T cell development by the transcription factor Foxp3. Science 299, 1057–1061. 10.1126/science.1079490. [PubMed: 12522256]
8. Fontenot JD, Gavin MA, and Rudensky AY (2003). Foxp3 programs the development and function of CD4+CD25+ regulatory T cells. Nat. Immunol. 4, 330–336. 10.1038/ni904. [PubMed: 12612578]
9. Bennett CL, Christie J, Ramsdell F, Brunkow ME, Ferguson PJ, Whitesell L, Kelly TE, Saulsbury FT, Chance PF, and Ochs HD (2001). The immune dysregulation, polyendocrinopathy, enteropathy, X-linked syndrome (IPEX) is caused by mutations of FOXP3. Nat. Genet. 27, 20–21. 10.1038/83713. [PubMed: 11137993]
10. Wildin RS, Ramsdell F, Peake J, Faravelli F, Casanova JL, Buist N, Levy-Lahad E, Mazzella M, Goulet O, Perroni L, et al. (2001). X-linked neonatal diabetes mellitus, enteropathy and endocrinopathy syndrome is the human equivalent of mouse scurfy. Nat. Genet. 27, 18–20. 10.1038/83707. [PubMed: 11137992]
11. Kim JM, Rasmussen JP, and Rudensky AY (2007). Regulatory T cells prevent catastrophic autoimmunity throughout the lifespan of mice. Nat. Immunol. 8, 191–197. 10.1038/ni1428. [PubMed: 17136045]
12. Atarashi K, Tanoue T, Shima T, Imaoka A, Kuwahara T, Momose Y, Cheng G, Yamasaki S, Saito T, Ohba Y, et al. (2011). Induction of colonic regulatory T cells by indigenous Clostridium species. Science 331, 337–341. 10.1126/science.1198469. [PubMed: 21205640]
13. Lathrop SK, Bloom SM, Rao SM, Nutsch K, Lio CW, Santacruz N, Peterson DA, Stappenbeck TS, and Hsieh CS (2011). Peripheral education of the immune system by colonic commensal microbiota. Nature 478, 250–254. 10.1038/nature10434. [PubMed: 21937990]
14. Nutsch K, Chai JN, Ai TL, Russler-Germain E, Feehley T, Nagler CR, and Hsieh CS (2016). Rapid and Efficient Generation of Regulatory T Cells to Commensal Antigens in the Periphery. Cell Rep. 17, 206–220. 10.1016/j.celrep.2016.08.092. [PubMed: 27681432]
15. Xu M, Pokrovskii M, Ding Y, Yi R, Au C, Harrison OJ, Galan C, Belkaid Y, Bonneau R, and Littman DR (2018). c-MAF-dependent regulatory T cells mediate immunological tolerance to a gut pathobiont. Nature 554, 373–377. 10.1038/nature25500. [PubMed: 29414937]

16. Atarashi K, Tanoue T, Oshima K, Suda W, Nagano Y, Nishikawa H, Fukuda S, Saito T, Narushima S, Hase K, et al. (2013). Treg induction by a rationally selected mixture of Clostridia strains from the human microbiota. Nature 500, 232–236. 10.1038/nature12331. [PubMed: 23842501]

17. Geuking MB, Cahenzli J, Lawson MAE, Ng DCK, Slack E, Hapfelmeier S, McCoy KD, and Macpherson AJ (2011). Intestinal bacterial colonization induces mutualistic regulatory T cell responses. Immunity 34, 794–806. 10.1016/j.immuni.2011.03.021. [PubMed: 21596591]

18. Chinen T, Volchkov PY, Chervonsky AV, and Rudensky AY (2010). A critical role for regulatory T cell-mediated control of inflammation in the absence of commensal microbiota. J. Exp. Med. 207, 2323–2330. 10.1084/jem.20101235. [PubMed: 20921284]

19. Holmén N, Lundgren A, Lundin S, Bergin AM, Rudin A, Sjövall H, and Ohman L (2006). Functional CD4+CD25high regulatory T cells are enriched in the colonic mucosa of patients with active ulcerative colitis and increase with disease activity. Inflamm. Bowel Dis. 12, 447–456. 10.1097/00054725-200606000-00003. [PubMed: 16775488]

20. Reikvam DH, Perminow G, Lyckander LG, Gran JM, Brandtzaeg P, Vatn M, and Carlsen HS (2011). Increase of regulatory T cells in ileal mucosa of untreated pediatric Crohn's disease patients. Scand. J. Gastroenterol. 46, 550–560. 10.3109/00365521.2011.551887. [PubMed: 21281255]

21. Yu QT, Saruta M, Avanesyan A, Fleshner PR, Banham AH, and Papadakis KA (2007). Expression and functional characterization of FOXP3+ CD4+ regulatory T cells in ulcerative colitis. Inflamm. Bowel Dis. 13, 191–199. 10.1002/ibd.20053. [PubMed: 17206665]

22. Ivanov II, Atarashi K, Manel N, Brodie EL, Shima T, Karaoz U, Wei D, Goldfarb KC, Santee CA, Lynch SV, et al. (2009). Induction of intestinal Th17 cells by segmented filamentous bacteria. Cell 139, 485–498. 10.1016/j.cell.2009.09.033. [PubMed: 19836068]

23. Yang Y, Torchinsky MB, Gobert M, Xiong H, Xu M, Linehan JL, Alonzo F, Ng C, Chen A, Lin X, et al. (2014). Focused specificity of intestinal TH17 cells towards commensal bacterial antigens. Nature 510, 152–156. 10.1038/nature13279. [PubMed: 24739972]

24. Shao TY, Ang WXG, Jiang TT, Huang FS, Andersen H, Kinder JM, Pham G, Burg AR, Ruff B, Gonzalez T, et al. (2019). Commensal Candida albicans Positively Calibrates Systemic Th17 Immunological Responses. Cell Host Microbe 25, 404–417.e6. 10.1016/j.chom.2019.02.004. [PubMed: 30870622]

25. Igyártó BZ, Haley K, Ortner D, Bobr A, Gerami-Nejad M, Edelson BT, Zurawski SM, Malissen B, Zurawski G, Berman J, and Kaplan DH (2011). Skin-resident murine dendritic cell subsets promote distinct and opposing antigen-specific T helper cell responses. Immunity 35, 260–272. 10.1016/j.immuni.2011.06.005. [PubMed: 21782478]

26. Jiang TT, Shao TY, Ang WXG, Kinder JM, Turner LH, Pham G, Whitt J, Alenghat T, and Way SS (2017). Commensal Fungi Recapitulate the Protective Benefits of Intestinal Bacteria. Cell Host Microbe 22, 809–816.e4. 10.1016/j.chom.2017.10.013. [PubMed: 29174402]

27. Moon JJ, Chu HH, Pepper M, McSorley SJ, Jameson SC, Kedl RM, and Jenkins MK (2007). Naive CD4(+) T cell frequency varies for different epitopes and predicts repertoire diversity and response magnitude. Immunity 27, 203–213. 10.1016/j.immuni.2007.07.007. [PubMed: 17707129]

28. Gutierrez D, Weinstock A, Antharam VC, Gu H, Jasbi P, Shi X, Dirks B, Krajmalnik-Brown R, Maldonado J, Guinan J, and Thangamani S (2020). Antibiotic-induced gut metabolome and microbiome alterations increase the susceptibility to Candida albicans colonization in the gastrointestinal tract. FEMS Microbiol. Ecol. 96, fiz187. 10.1093/femsec/fiz187. [PubMed: 31769789]

29. Baaten BJG, Tinoco R, Chen AT, and Bradley LM (2012). Regulation of Antigen-Experienced T Cells: Lessons from the Quintessential Memory Marker CD44. Front. Immunol. 3, 23. 10.3389/fimmu.2012.00023. [PubMed: 22566907]

30. Ertelt JM, Rowe JH, Johanns TM, Lai JC, McLachlan JB, and Way SS (2009). Selective priming and expansion of antigen-specific Foxp3- CD4+ T cells during Listeria monocytogenes infection. J. Immunol. 182, 3032–3038. 10.4049/jimmunol.0803402. [PubMed: 19234199]

31. Benoun JM, Peres NG, Wang N, Pham OH, Rudisill VL, Fogassy ZN, Whitney PG, Fernandez-Ruiz D, Gebhardt T, Pham QM, et al. (2018). Optimal protection against Salmonella infection requires noncirculating memory. Proc. Natl. Acad. Sci. USA 115, 10416–10421. 10.1073/pnas.1808339115. [PubMed: 30254173]

32. Carlson CM, Endrizzi BT, Wu J, Ding X, Weinreich MA, Walsh ER, Wani MA, Lingrel JB, Hogquist KA, and Jameson SC (2006). Kruppel-like factor 2 regulates thymocyte and T-cell migration. Nature 442, 299–302. 10.1038/nature04882. [PubMed: 16855590]
33. Sebzda E, Zou Z, Lee JS, Wang T, and Kahn ML (2008). Transcription factor KLF2 regulates the migration of naive T cells by restricting chemokine receptor expression patterns. Nat. Immunol. 9, 292–300. 10.1038/ni1565. [PubMed: 18246069]
34. Weinreich MA, Takada K, Skon C, Reiner SL, Jameson SC, and Hogquist KA (2009). KLF2 transcription-factor deficiency in T cells results in unrestrained cytokine production and upregulation of bystander chemokine receptors. Immunity 31, 122–130. 10.1016/j.immuni.2009.05.011. [PubMed: 19592277]
35. Hong SW, Krueger PD, Osum KC, Dileepan T, Herman A, Mueller DL, and Jenkins MK (2022). Immune tolerance of food is mediated by layers of CD4(+) T cell dysfunction. Nature 607, 762–768. 10.1038/s41586-022-04916-6. [PubMed: 35794484]
36. Hepworth MR, Fung TC, Masur SH, Kelsen JR, McConnell FM, Dubrot J, Withers DR, Hugues S, Farrar MA, Reith W, et al. (2015). Immune tolerance. Group 3 innate lymphoid cells mediate intestinal selection of commensal bacteria-specific CD4(+) T cells. Science 348, 1031–1035. 10.1126/science.aaa4812. [PubMed: 25908663]
37. Cong Y, Feng T, Fujihashi K, Schoeb TR, and Elson CO (2009). A dominant, coordinated T regulatory cell-IgA response to the intestinal microbiota. Proc. Natl. Acad. Sci. USA 106, 19256–19261. 10.1073/pnas.0812681106. [PubMed: 19889972]
38. Feng T, Cao AT, Weaver CT, Elson CO, and Cong Y (2011). Interleukin-12 converts Foxp3+ regulatory T cells to interferon-gamma-producing Foxp3+ T cells that inhibit colitis. Gastroenterology 140, 2031–2043. 10.1053/j.gastro.2011.03.009. [PubMed: 21419767]
39. Abt MC, Osborne LC, Monticelli LA, Doering TA, Alenghat T, Sonnenberg GF, Paley MA, Antenus M, Williams KL, Erikson J, et al. (2012). Commensal bacteria calibrate the activation threshold of innate antiviral immunity. Immunity 37, 158–170. 10.1016/j.immuni.2012.04.011. [PubMed: 22705104]
40. Elahi S, Ertelt JM, Kinder JM, Jiang TT, Zhang X, Xin L, Chaturvedi V, Strong BS, Qualls JE, Steinbrecher KA, et al. (2013). Immunosuppressive CD71+ erythroid cells compromise neonatal host defence against infection. Nature 504, 158–162. 10.1038/nature12675. [PubMed: 24196717]
41. Lee PP, Fitzpatrick DR, Beard C, Jessup HK, Lehar S, Makar KW, Pérez-Melgosa M, Sweetser MT, Schlissel MS, Nguyen S, et al. (2001). A critical role for Dnmt1 and DNA methylation in T cell development, function, and survival. Immunity 15, 763–774. 10.1016/s1074-7613(01)00227-8. [PubMed: 11728338]
42. Lingrel JB, Pilcher-Roberts R, Basford JE, Manoharan P, Neumann J, Konaniah ES, Srinivasan R, Bogdanov VY, and Hui DY (2012). Myeloid-specific Kruppel-like factor 2 inactivation increases macrophage and neutrophil adhesion and promotes atherosclerosis. Circ. Res. 110, 1294–1302. 10.1161/CIRCRESAHA.112.267310. [PubMed: 22474254]
43. Chassaing B, Srinivasan G, Delgado MA, Young AN, Gewirtz AT, and Vijay-Kumar M (2012). Fecal lipocalin 2, a sensitive and broadly dynamic non-invasive biomarker for intestinal inflammation. PLoS One 7, e44328. 10.1371/journal.pone.0044328. [PubMed: 22957064]
44. Pabbisetty SK, Rabacal W, Maseda D, Cendron D, Collins PL, Hoek KL, Parekh VV, Aune TM, and Sebzda E (2014). KLF2 is a rate-limiting transcription factor that can be targeted to enhance regulatory T-cell production. Proc. Natl. Acad. Sci. USA 111, 9579–9584. 10.1073/pnas.1323493111. [PubMed: 24979767]
45. Pabbisetty SK, Rabacal W, Volanakis EJ, Parekh VV, Olivares-Villagómez D, Cendron D, Boyd KL, Van Kaer L, and Sebzda E (2016). Peripheral tolerance can be modified by altering KLF2-regulated Treg migration. Proc. Natl. Acad. Sci. USA 113, E4662–E4670. 10.1073/pnas.1605849113. [PubMed: 27462110]
46. Thornton AM, and Shevach EM (1998). CD4+CD25+ immunoregulatory T cells suppress polyclonal T cell activation in vitro by inhibiting interleukin 2 production. J. Exp. Med. 188, 287–296. 10.1084/jem.188.2.287. [PubMed: 9670041]
47. Fontenot JD, Rasmussen JP, Williams LM, Dooley JL, Farr AG, and Rudensky AY (2005). Regulatory T cell lineage specification by the forkhead transcription factor foxp3. Immunity 22, 329–341. 10.1016/j.immuni.2005.01.016. [PubMed: 15780990]

48. Powrie F, Leach MW, Mauze S, Caddle LB, and Coffman RL (1993). Phenotypically distinct subsets of CD4+ T cells induce or protect from chronic intestinal inflammation in C. B-17 scid mice. Int. Immunol. 5, 1461–1471. 10.1093/intimm/5.11.1461. [PubMed: 7903159]
49. Mottet C, Uhlig HH, and Powrie F (2003). Cutting edge: cure of colitis by CD4+CD25+ regulatory T cells. J. Immunol. 170, 3939–3943. 10.4049/jimmunol.170.8.3939. [PubMed: 12682220]
50. Ostanin DV, Bao J, Koboziev I, Gray L, Robinson-Jackson SA, Kosloski-Davidson M, Price VH, and Grisham MB (2009). T cell transfer model of chronic colitis: concepts, considerations, and tricks of the trade. Am. J. Physiol. Gastrointest. Liver Physiol 296, G135–G146. 10.1152/ajpgi.90462.2008. [PubMed: 19033538]
51. McPherson SW, Heuss ND, Pierson MJ, and Gregerson DS (2014). Retinal antigen-specific regulatory T cells protect against spontaneous and induced autoimmunity and require local dendritic cells. J. Neuroinflammation 11, 205. 10.1186/s12974-014-0205-4. [PubMed: 25498509]
52. Kühn R, Löhler J, Rennick D, Rajewsky K, and Müller W (1993). Interleukin-10-deficient mice develop chronic enterocolitis. Cell 75, 263–274. 10.1016/0092-8674(93)80068-. [PubMed: 8402911]
53. Madsen KL, Doyle JS, Tavernini MM, Jewell LD, Rennie RP, and Fedorak RN (2000). Antibiotic therapy attenuates colitis in interleukin 10 gene-deficient mice. Gastroenterology 118, 1094–1105. 10.1016/s0016-5085(00)70362-3. [PubMed: 10833484]
54. Sellon RK, Tonkonogy S, Schultz M, Dieleman LA, Grenther W, Balish E, Rennick DM, and Sartor RB (1998). Resident enteric bacteria are necessary for development of spontaneous colitis and immune system activation in interleukin-10-deficient mice. Infect. Immun. 66, 5224–5231. 10.1128/IAI.66.11.5224-5231.1998. [PubMed: 9784526]
55. Maynard CL, Harrington LE, Janowski KM, Oliver JR, Zindl CL, Rudensky AY, and Weaver CT (2007). Regulatory T cells expressing interleukin 10 develop from Foxp3+ and Foxp3− precursor cells in the absence of interleukin 10. Nat. Immunol. 8, 931–941. 10.1038/ni1504. [PubMed: 17694059]
56. Roncarolo MG, Gregori S, Bacchetta R, Battaglia M, and Gagliani N (2018). The Biology of T Regulatory Type 1 Cells and Their Therapeutic Application in Immune-Mediated Diseases. Immunity 49, 1004–1019. 10.1016/j.immuni.2018.12.001. [PubMed: 30566879]
57. Levings MK, Bacchetta R, Schulz U, and Roncarolo MG (2002). The role of IL-10 and TGF-beta in the differentiation and effector function of T regulatory cells. Int. Arch. Allergy Immunol. 129, 263–276. 10.1159/000067596. [PubMed: 12483031]
58. Gagliani N, Magnani CF, Huber S, Gianolini ME, Pala M, Licona-Limon P, Guo B, Herbert DR, Bulfone A, Trentini F, et al. (2013). Co-expression of CD49b and LAG-3 identifies human and mouse T regulatory type 1 cells. Nat. Med. 19, 739–746. 10.1038/nm.3179. [PubMed: 23624599]
59. Akbari O, Freeman GJ, Meyer EH, Greenfield EA, Chang TT, Sharpe AH, Berry G, DeKruyff RH, and Umetsu DT (2002). Antigen-specific regulatory T cells develop via the ICOS-ICOS-ligand pathway and inhibit allergen-induced airway hyperreactivity. Nat. Med. 8, 1024–1032. 10.1038/nm745. [PubMed: 12145647]
60. Kohyama M, Sugahara D, Sugiyama S, Yagita H, Okumura K, and Hozumi N (2004). Inducible costimulator-dependent IL-10 production by regulatory T cells specific for self-antigen. Proc. Natl. Acad. Sci. USA 101, 4192–4197. 10.1073/pnas.0400214101. [PubMed: 15014176]
61. Chen PP, Cepika AM, Agarwal-Hashmi R, Saini G, Uyeda MJ, Louis DM, Cieniewicz B, Narula M, Amaya Hernandez LC, Harre N, et al. (2021). Alloantigen-specific type 1 regulatory T cells suppress through CTLA-4 and PD-1 pathways and persist long-term in patients. Sci. Transl. Med. 13, eabf5264. 10.1126/scitranslmed.abf5264. [PubMed: 34705520]
62. Groux H, O'Garra A, Bigler M, Rouleau M, Antonenko S, de Vries JE, and Roncarolo MG (1997). A CD4+ T-cell subset inhibits antigen-specific T-cell responses and prevents colitis. Nature 389, 737–742. 10.1038/39614. [PubMed: 9338786]
63. Brinkmann V, Cyster JG, and Hla T (2004). FTY720: sphingosine 1-phosphate receptor-1 in the control of lymphocyte egress and endothelial barrier function. Am. J. Transplant. 4, 1019–1025. 10.1111/j.1600-6143.2004.00476.x. [PubMed: 15196057]

64. Cyster JG, and Schwab SR (2012). Sphingosine-1-phosphate and lymphocyte egress from lymphoid organs. Annu. Rev. Immunol. 30, 69–94. 10.1146/annurev-immunol-020711-075011. [PubMed: 22149932]

65. Blander JM, Longman RS, Iliev ID, Sonnenberg GF, and Artis D (2017). Regulation of inflammation by microbiota interactions with the host. Nat. Immunol. 18, 851–860. 10.1038/ni.3780. [PubMed: 28722709]

66. Chang JT (2020). Pathophysiology of Inflammatory Bowel Diseases. N. Engl. J. Med. 383, 2652–2664. 10.1056/NEJMra2002697. [PubMed: 33382932]

67. Iliev ID, and Cadwell K (2021). Effects of Intestinal Fungi and Viruses on Immune Responses and Inflammatory Bowel Diseases. Gastroenterology 160, 1050–1066. 10.1053/j.gastro.2020.06.100. [PubMed: 33347881]

68. Elmentaite R, Ross ADB, Roberts K, James KR, Ortmann D, Gomes T, Nayak K, Tuck L, Pritchard S, Bayraktar OA, et al. (2020). Single-Cell Sequencing of Developing Human Gut Reveals Transcriptional Links to Childhood Crohn's Disease. Dev. Cell 55, 771–783.e5. 10.1016/j.devcel.2020.11.010. [PubMed: 33290721]

69. Jaeger N, Gamini R, Cella M, Schettini JL, Bugatti M, Zhao S, Rosadini CV, Esaulova E, Di Luccia B, Kinnett B, et al. (2021). Single-cell analyses of Crohn's disease tissues reveal intestinal intraepithelial T cells heterogeneity and altered subset distributions. Nat. Commun. 12, 1921. 10.1038/s41467-021-22164-6. [PubMed: 33771991]

70. Martin JC, Chang C, Boschetti G, Ungaro R, Giri M, Grout JA, Gettler K, Chuang LS, Nayar S, Greenstein AJ, et al. (2019). Single-Cell Analysis of Crohn's Disease Lesions Identifies a Pathogenic Cellular Module Associated with Resistance to Anti-TNF Therapy. Cell 178, 1493–1508.e20. 10.1016/j.cell.2019.08.008. [PubMed: 31474370]

71. Ronchetti S, Migliorati G, and Riccardi C (2015). GILZ as a Mediator of the Anti-Inflammatory Effects of Glucocorticoids. Front. Endocrinol. 6, 170. 10.3389/fendo.2015.00170.

72. Suk FM, Chang CC, Lin RJ, Lin SY, Liu SC, Jau CF, and Liang YC (2018). ZFP36L1 and ZFP36L2 inhibit cell proliferation in a cyclin D-dependent and p53-independent manner. Sci. Rep. 8, 2742. 10.1038/s41598-018-21160-z. [PubMed: 29426877]

73. Rauen T, Hedrich CM, Juang YT, Tenbrock K, and Tsokos GC (2011). cAMP-responsive element modulator (CREM)alpha protein induces interleukin 17A expression and mediates epigenetic alterations at the interleukin-17A gene locus in patients with systemic lupus erythematosus. J. Biol. Chem. 286, 43437–43446. 10.1074/jbc.M111.299313. [PubMed: 22025620]

74. Kröger A (2017). IRFs as competing pioneers in T-cell differentiation. Cell. Mol. Immunol. 14, 649–651. 10.1038/cmi.2017.37. [PubMed: 28626239]

75. Brestoff JR, and Artis D (2013). Commensal bacteria at the interface of host metabolism and the immune system. Nat. Immunol. 14, 676–684. 10.1038/ni.2640. [PubMed: 23778795]

76. Chow J, Lee SM, Shen Y, Khosravi A, and Mazmanian SK (2010). Host-bacterial symbiosis in health and disease. Adv. Immunol. 107, 243–274. 10.1016/B978-0-12-381300-8.00008-3. [PubMed: 21034976]

77. Rubtsov YP, Rasmussen JP, Chi EY, Fontenot J, Castelli L, Ye X, Treuting P, Siewe L, Roers A, Henderson WR Jr., et al. (2008). Regulatory T cell-derived interleukin-10 limits inflammation at environmental interfaces. Immunity 28, 546–558. 10.1016/j.immuni.2008.02.017. [PubMed: 18387831]

78. Cheng SB, and Sharma S (2015). Interleukin-10: a pleiotropic regulator in pregnancy. Am. J. Reprod. Immunol. 73, 487–500. 10.1111/aji.12329. [PubMed: 25269386]

79. Cyktor JC, and Turner J (2011). Interleukin-10 and immunity against prokaryotic and eukaryotic intracellular pathogens. Infect. Immun. 79, 2964–2973. 10.1128/IAI.00047-11. [PubMed: 21576331]

80. Erickson JJ, Archer-Hartmann S, Yarawsky AE, Miller JLC, Seveau S, Shao TY, Severance AL, Miller-Handley H, Wu Y, Pham G, et al. (2022). Pregnancy enables antibody protection against intracellular infection. Nature 606, 769–775. 10.1038/s41586-022-04816-9. [PubMed: 35676476]

81. Shao TY, Kinder JM, Harper G, Pham G, Peng Y, Liu J, Gregory EJ, Sherman BE, Wu Y, Iten AE, et al. (2023). Reproductive outcomes after pregnancy-induced displacement of preexisting microchimeric cells. Science 381, 1324–1330. 10.1126/science.adf9325. [PubMed: 37733857]

82. Liao Y, Smyth GK, and Shi W (2019). The R package Rsubread is easier, faster, cheaper and better for alignment and quantification of RNA sequencing reads. Nucleic Acids Res. 47, e47. 10.1093/nar/gkz114. [PubMed: 30783653]

83. Love MI, Huber W, and Anders S (2014). Moderated estimation of fold change and dispersion for RNA-seq data with DESeq2. Genome Biol. 15, 550. 10.1186/s13059-014-0550-8. [PubMed: 25516281]

84. Eshleman EM, Shao TY, Woo V, Rice T, Engleman L, Didriksen BJ, Whitt J, Haslam DB, Way SS, and Alenghat T (2023). Intestinal epithelial HDAC3 and MHC class II coordinate microbiota-specific immunity. J. Clin. Invest. 133, e162190. 10.1172/JCI162190. [PubMed: 36602872]

85. Wan YY, and Flavell RA (2005). Identifying Foxp3-expressing suppressor T cells with a bicistronic reporter. Proc. Natl. Acad. Sci. USA. 102, 5126–5131. 10.1073/pnas.0501701102. [PubMed: 15795373]

86. Aghajani K, Keerthivasan S, Yu Y, and Gounari F (2012). Generation of CD4CreER(T(2)) transgenic mice to study development of peripheral CD4-T-cells. Genesis 50, 908–913. 10.1002/dvg.22052. [PubMed: 22887772]

87. Chen CY, Lee JB, Liu B, Ohta S, Wang PY, Kartashov AV, Mugge L, Abonia JP, Barski A, Izuhara K, et al. (2015). Induction of Interleukin-9-Producing Mucosal Mast Cells Promotes Susceptibility to IgE-Mediated Experimental Food Allergy. Immunity 43, 788–802. 10.1016/j.immuni.2015.08.020. [PubMed: 26410628]

88. Navabi N, Whitt J, Wu SE, Woo V, Moncivaiz J, Jordan MB, Vallance BA, Way SS, and Alenghat T (2017). Epithelial Histone Deacetylase 3 Instructs Intestinal Immunity by Coordinating Local Lymphocyte Activation. Cell Rep. 19, 1165–1175. 10.1016/j.celrep.2017.04.046. [PubMed: 28494866]

89. Huber S, Gagliani N, Esplugues E, O'Connor W Jr., Huber FJ, Chaudhry A, Kamanaka M, Kobayashi Y, Booth CJ, Rudensky AY, et al. (2011). Th17 cells express interleukin-10 receptor and are controlled by Foxp3(−) and Foxp3+ regulatory CD4+ T cells in an interleukin-10-dependent manner. Immunity 34, 554–565. 10.1016/j.immuni.2011.01.020. [PubMed: 21511184]

90. Lee JY, Skon CN, Lee YJ, Oh S, Taylor JJ, Malhotra D, Jenkins MK, Rosenfeld MG, Hogquist KA, and Jameson SC (2015). The transcription factor KLF2 restrains CD4(+) T follicular helper cell differentiation. Immunity 42, 252–264. 10.1016/j.immuni.2015.01.013. [PubMed: 25692701]

91. Satija R, Farrell JA, Gennert D, Schier AF, and Regev A (2015). Spatial reconstruction of single-cell gene expression data. Nat. Biotechnol. 33, 495–502. 10.1038/nbt.3192. [PubMed: 25867923]

92. Dobin A, Davis CA, Schlesinger F, Drenkow J, Zaleski C, Jha S, Batut P, Chaisson M, and Gingeras TR (2013). STAR: ultrafast universal RNA-seq aligner. Bioinformatics 29, 15–21. 10.1093/bioinformatics/bts635. [PubMed: 23104886]

93. Smillie CS, Biton M, Ordovas-Montanes J, Sullivan KM, Burgin G, Graham DB, Herbst RH, Rogel N, Slyper M, Waldman J, et al. (2019). Intra- and Inter-cellular Rewiring of the Human Colon during Ulcerative Colitis. Cell 178, 714–730.e22. 10.1016/j.cell.2019.06.029. [PubMed: 31348891]

94. Hao Y, Hao S, Andersen-Nissen E, Mauck WM 3rd, Zheng S, Butler A, Lee MJ, Wilk AJ, Darby C, Zager M, et al. (2021). Integrated analysis of multimodal single-cell data. Cell 184, 3573–3587.e29. 10.1016/j.cell.2021.04.048. [PubMed: 34062119]

95. Mi H, Muruganujan A, Huang X, Ebert D, Mills C, Guo X, and Thomas PD (2019). Protocol Update for large-scale genome and gene function analysis with the PANTHER classification system (v.14.0). Nat. Protoc. 14, 703–721. 10.1038/s41596-019-0128-8. [PubMed: 30804569]

Highlights

- Microbiota-primed lineage-negative CD4 T cells are unified by KLF2 expression
- Loss of KLF2 in CD4 cells causes microbiota-driven intestinal inflammation
- Activated KLF2+ CD4 cells exert immune regulation via IL-10 cytokine production
- Reduced KLF2+ CD4 T cells in human Crohn’s disease inflamed tissue

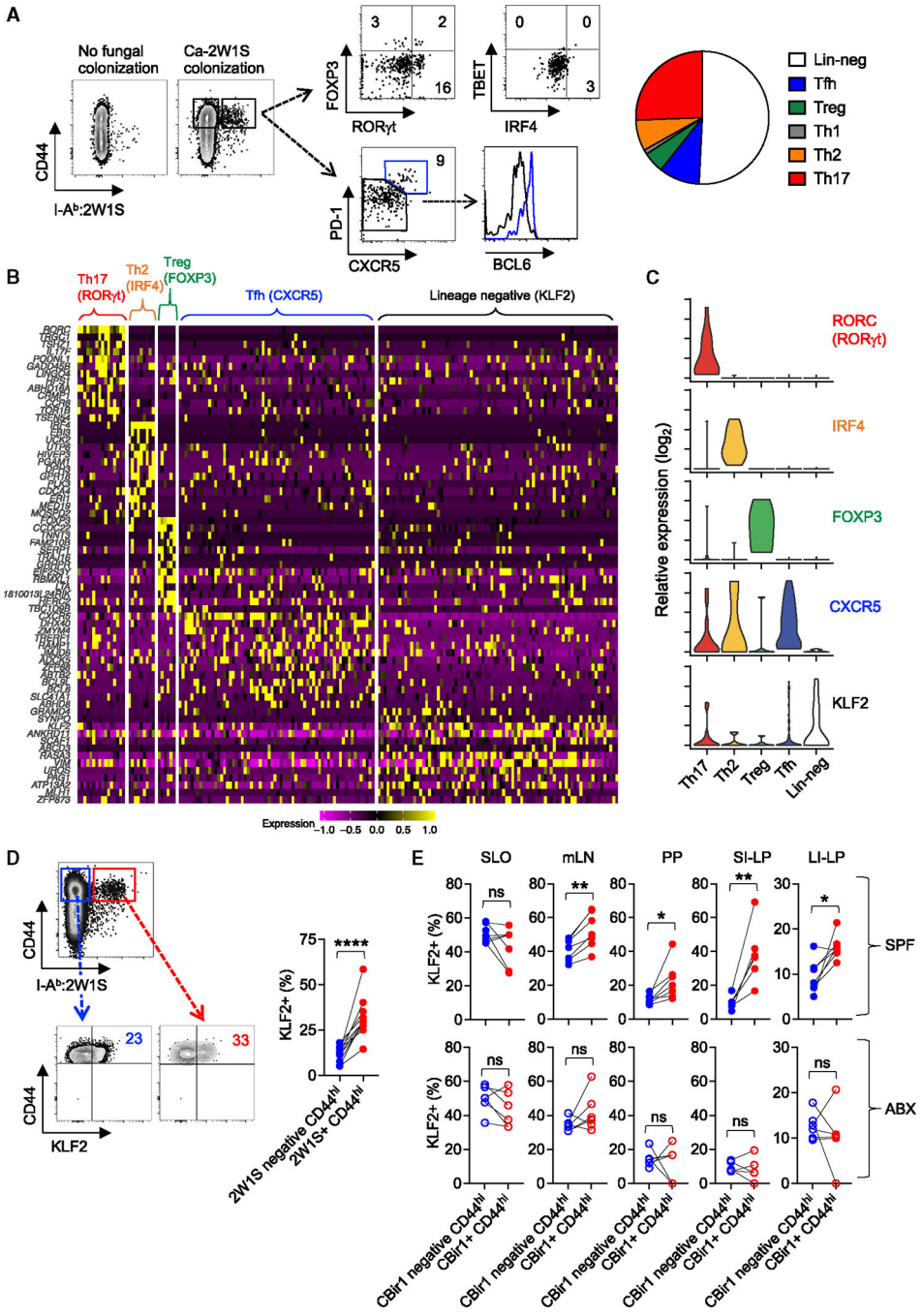

Figure 1. Commensal stimulation primes lineage-negative CD4 cells specified by KLF2 expression

(A) Expansion of CD44^{hi} CD4 cells in the spleen and peripheral lymph nodes with I-A^{b}:2W1S$_{55–68}$ commensal Ca-2W1S specificity after intestinal colonization, and their expression of lineage-defining markers including FOXP3 (Tregs), RORγt (Th17), TBET (Th1), IRF4 (Th2), and PD-1/CXCR5/BCL6 (Tfh).

(B) Single-cell gene expression profiling of commensal Ca-2W1S I-A^{b}:2W1S$_{55–68}$ CD44^{hi} CD4 cells in the spleen and peripheral lymph nodes based on expression of lineage-defining

markers (RORC for Th17, IRF4 for Th2, CXCR5 for Tfh, and FOXP3 for Treg), with the remaining unaccounted lineage-negative cells unified by KLF2 expression.

(C) Relative expression of each lineage-defining marker and KLF2 by cells in each cluster identified in (B).

(D) KLF2 expression by $CD44^{hi}$ CD4 cells in the spleen and peripheral lymph nodes with $I\text{-}A^{b}$:$2W1S_{55–68}$ surrogate commensal specificity in Ca-2W1S-colonized KLF2(GFP) reporter mice compared with tetramer-negative cells of irrelevant bulk specificity.

(E) KLF2 expression by $CD44^{hi}$ CD4 cells isolated from each tissue with $I\text{-}A^{b}$:$CBir1_{464–472}$ specificity in KLF2(GFP) reporter mice compared with tetramer-negative cells of irrelevant bulk specificity. SLO, secondary lymphoid organ; mLN, mesenteric lymph node; PP, Peyer patch; SI-LP, small intestine lamina propria; LI-LP, large intestine lamina propria; SPF, specific pathogen free; ABX, drinking water supplementation with five antibiotics (ampicillin, gentamicin, metronidazole, neomycin, vancomycin) to eliminate commensal bacteria. Each point indicates the data from an individual mouse, and these results represent data from at least five independently colonized mice and two independent experiments each with similar results. *$p < 0.05$, **$p < 0.01$, ****$p < 0.001$, using paired t test; ns, not significant. See also Figures S1, S2, and S3 and Table S1.

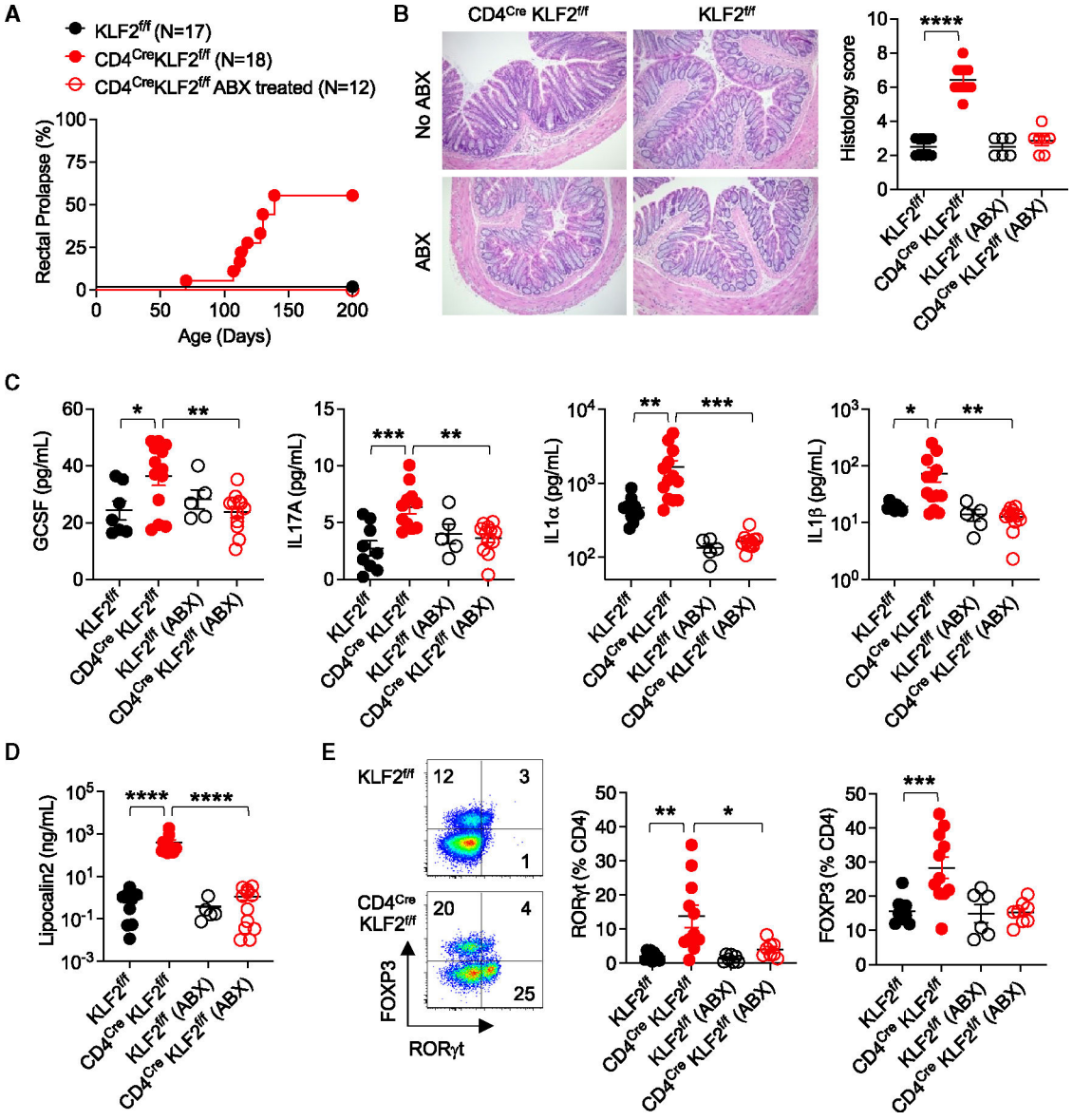

Figure 2. Spontaneous colitis in mice lacking KLF2+ CD4 cells

(A) Rectal prolapse incidence in CD4^{Cre} KLF2$^{f/f}$ (filled red) compared with co-housed KLF2$^{f/f}$ littermate controls (black), or for CD4^{Cre} KLF2$^{f/f}$ mice administered antibiotics (ampicillin, gentamicin, metronidazole, neomycin, vancomycin) in the drinking water beginning at age 40 days (open red).

(B) Colonic histology and inflammation scoring for CD4^{Cre} KLF2$^{f/f}$ mice that did not develop rectal prolapse through 150 days of age (red) compared with co-housed KLF2$^{f/f}$ littermate control mice (black), with some mice in each group administered antibiotics as described in (A) (open circles).

(C) Fecal levels of each cytokine for each group of mice described in (B).

(D) Fecal Lipocalin2 levels for each group of mice described in (B).

(E) Percent RORγt- and FOXP3-expressing mLN CD4 cells for each group of mice described in (B). Each point indicates the data from an individual mouse, combined from at

least two independent experiments each with similar results. *p < 0.05, **p < 0.01, ***p < 0.005, ****p < 0.001, using one-way ANOVA; bar, mean ± SEM. See also Figure S4.

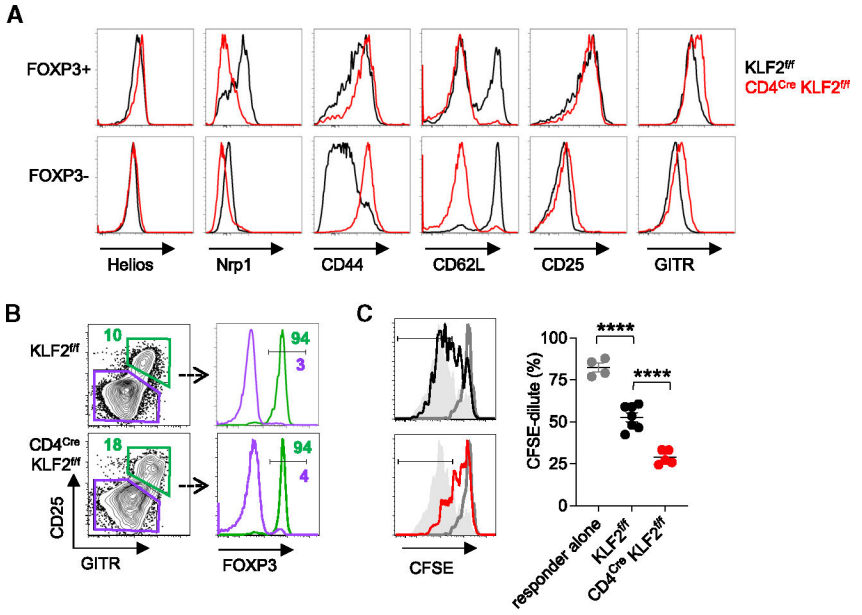

Figure 3. Enhanced suppressive function by GITR+ CD25+ Tregs expanded in CD4^{Cre} KLF2$^{f/f}$ mice

(A) Phenotypic comparison of FOXP3+ and FOXP3-negative mLN CD4 cells in CD4^{Cre} KLF2$^{f/f}$ (red) compared with Cre-negative littermate control mice (black).

(B) Representative plots showing GITR and CD25 expression by mLN CD4 cells in CD4^{Cre} KLF2$^{f/f}$ or Cre-negative littermate controls, and FOXP3 expression by GITR+ CD25+ (green) compared with GITR-negative CD25-negative (purple) cells from each group of mice.

(C) CFSE dilution by responder CD4 splenocytes afteranti-CD3/CD28 stimulation (96 h) and co-culture with purified GITR+ CD25+ mLN CD4 cells from CD4^{Cre} KLF2$^{f/f}$ (red) compared with GITR+ CD25+ mLN CD4 cells from Cre-negative control mice (black) each at a 1:1 ratio, or responder cells alone (gray). Each point indicates the data from an individual mouse, combined from at least two independent experiments each with similar results. ****$p < 0.001$, using one-way ANOVA; bar, mean ± SEM.

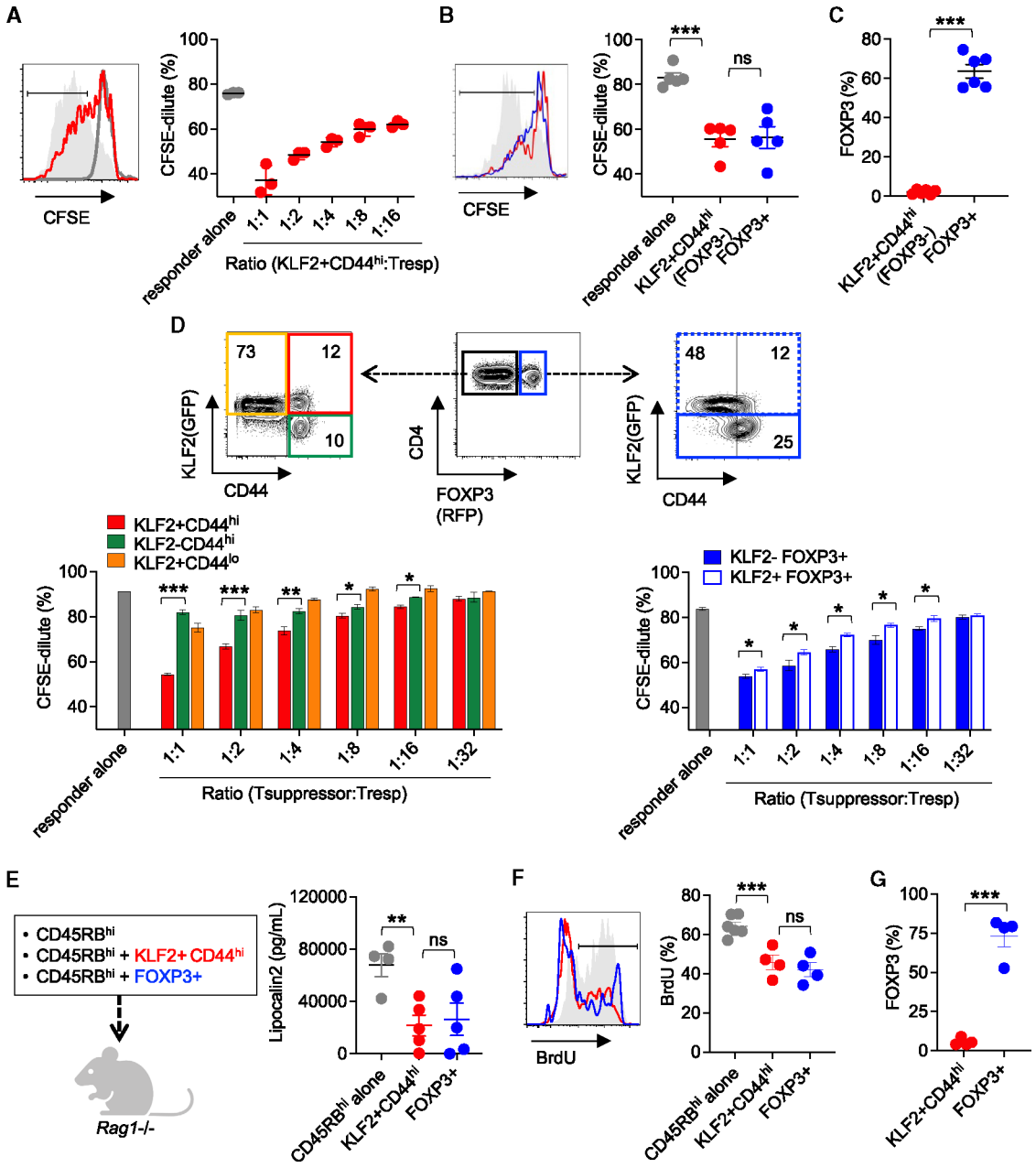

Figure 4. KLF2 identifies antigen-experienced suppressive FOXP3-negative CD4 cells

(A) CFSE dilution by responder CD4 splenocytes after anti-CD3/CD28 stimulation (96 h) and co-culture with purified KLF2+ CD44^{hi} CD4 splenocytes at each ratio (red), anti-CD3/CD28-stimulated responder cells alone (gray filled), or responder cells without stimulation (gray line).

(B) CFSE dilution by responder CD4 splenocytes after anti-CD3/CD28 stimulation (96 h) and co-culture with purified FOXP3-negative KLF2+ CD44^{hi} (red) compared with FOXP3+ (blue) CD4 splenocytes each at a 1:1 ratio, or anti-CD3/CD28-stimulated responder cells alone (gray).

(C) Percent FOXP3+ among purified FOXP3-negative KLF2+ CD44^{hi} (red) compared with FOXP3+ (blue) CD4 cells after anti-CD3/CD28 stimulation, and co-culture with responder cells as described in (B).

(D) CFSE dilution by responder CD4 splenocytes after anti-CD3/CD28 stimulation (96 h) and co-culture with each subset of FOXP3-negative cells including KLF2+ CD44^{hi} (red), KLF2-negative CD44^{hi} (green), and KLF2+ CD44^{lo} (orange) cells, or FOXP3+ cells including KLF2+ (blue dotted) compared with KLF2-negative (blue line) cells at each ratio compared with anti-CD3/CD28-stimulated responder cells alone (gray).

(E) Fecal Lipocalin2 levels day 20 after transfer of CD45RB^{hi} cells (5×10^4 cells; CD45.1 congenic) into *Rag1−/−* recipient mice (gray), or *Rag1−/−* mice co-transferred CD45RB^{hi} cells with purified KLF2+ CD44^{hi} (FOXP3-negative) (5×10^5 cells; red) or FOXP3+ cells (5×10^5 cells; blue).

(F) BrdU incorporation by mLN CD45RB^{hi} CD45.1 donor cells for the mice described in (E).

(G) FOXP3 expression by mLN KLF2+ CD44^{hi} (FOXP3-negative) (red) or FOXP3+ cells (blue) (CD45.1-negative, CD45.2-positive) donor CD4 cells for the mice described in (E). Each point indicates the data from an individual mouse, combined from at least two independent experiments each with similar results. *$p < 0.05$, **$p < 0.01$, ***$p < 0.005$ using one-way ANOVA for multiple groups or unpaired t test for two groups; bar, mean ± SEM; dotted line, limit of detection. See also Figure S5.

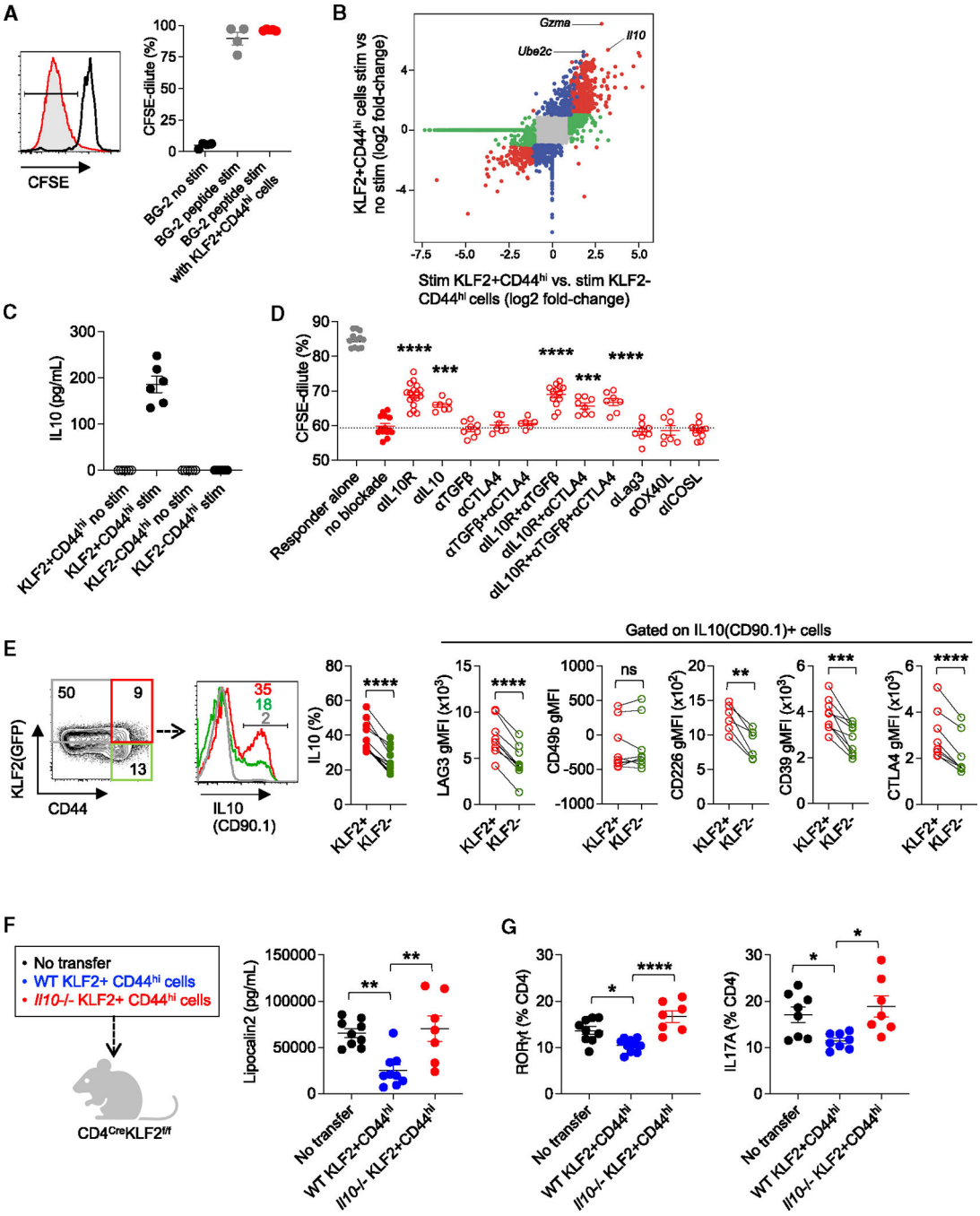

Figure 5. KLF2+ cells selective produce and utilize IL-10 for *in vitro* and *in vivo* suppression

(A) CFSE dilution by responder CD4 splenocytes from BG2 TCR transgenic mice without stimulation (black), after β-gal peptide stimulation (gray), or β-gal peptide stimulation plus co-culture (96 h) with purified FOXP3-negative KLF2+ CD44^{hi} cells (red) at a 1:1 ratio. (B) Differential gene expression by KLF2+ CD44^{hi} (FOXP3-negative) cells upon anti-CD3/CD28 stimulation (48 h) compared with no simulation controls (y axis), and differential gene expression by KLF2+ CD44^{hi} (FOXP3-negative) compared with KLF2-negative CD44^{hi} (FOXP3-negative) cells after stimulation (x axis); with genes significantly different

($p < 0.05$) between KLF2+ CD44^{hi} cells after stimulation compared with no simulation controls highlighted in blue, genes significantly different between KLF2+ CD44^{hi} (FOXP3-negative) compared with KLF2-negative CD44^{hi} (FOXP3-negative) cells after stimulation highlighted in green, and those significantly different in both parameters highlighted in red.
(C) IL-10 concentration in culture supernatants of purified KLF2+ compared with KLF2-negative CD44^{hi} FOXP3-negative cells after anti-CD3/CD28 stimulation as described in (B).
(D) CFSE dilution by responder CD4 cells after anti-CD3/CD28 stimulation (96 h) and co-culture with purified KLF2+ CD44^{hi} FOXP3-negative CD4 cells at a 1:1 ratio with medium supplemented with neutralizing antibodies against each cytokine or cell-associated molecule with statistics compared with no-blockade (isotype treatment) controls.
(E) Representative plots and composite data showing IL-10 (CD90.1) expression by FOXP3-negative splenic CD4 cells from triple reporter (10BiT, IL-10[CD90.1];KLF2[GFP]; FOXP3[RFP]) mice after anti-CD3 stimulation, and expression of each Tr1-associated marker by IL-10-producing KLF2+ compared with KLF2-negative cells.
(F) Fecal Lipocalin2 levels in CD4^{Cre} KLF2$^{f/f}$ recipient mice day 20 after transfer of KLF2+ CD44^{hi} (FOXP3-negative) cells from WT (10^6 cells; blue) or *Il10*−/− donors (10^6 cells; red) compared with no transfer controls (black).
(G) Percent RORγt+ or IL-17A+ after PMA-ionomycin stimulation by mLN CD4 cells for each group of mice described in (F). Each point indicates the data from an individual mouse, combined from at least two independent experiments each with similar results. *$p < 0.05$, **$p < 0.01$, ***$p < 0.005$, ****$p < 0.001$ using one-way ANOVA for multiple groups or paired t test for two groups; bar, mean ± SEM. See also Figure S6 and Table S2.

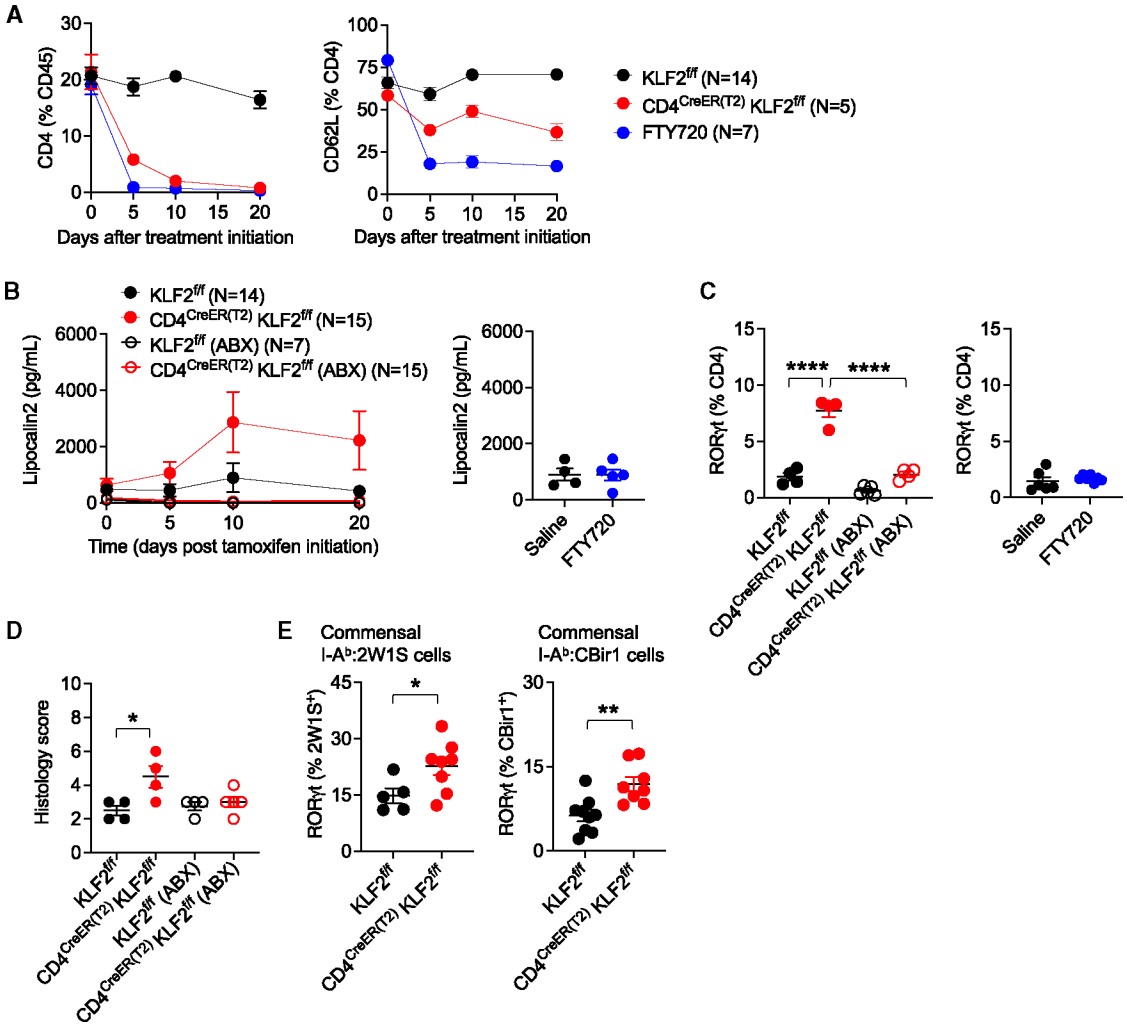

Figure 6. Dissociating peripheral lymphopenia from intestinal inflammation with induced KLF2 deficiency in CD4 cells

(A) Percent CD4 cells among $CD45^+$ leukocytes in the peripheral blood and their expression of CD62L for $CD4^{CreER(T2)}$ $KLF2^{f/f}$ mice (red) or Cre-negative littermate controls (black) after initiating tamoxifen supplemented chow, compared with isogenic C57BL/6 control mice after initiating daily administration of the S1PR1 modulator FTY720 (20 μg IP; blue).

(B) Fecal Lipocalin2 levels after initiating tamoxifen supplemented chow to $CD4^{CreER(T2)}$ KLF2-floxed (red) or Cre-negative control (black) mice at age 6–8 weeks, with some mice in each group administered antibiotics (ampicillin, gentamicin, metronidazole, neomycin, vancomycin) in the drinking water (open), compared with mice day 20 after daily administration of the S1PR1 modulator FTY720 (blue).

(C) Percent RORγt+ mLN CD4 cells for each group of mice described in (A) 25 days after initiating tamoxifen supplemented chow with or without additional drinking water antibiotic supplementation, compared with mice day 25 after daily administration of the S1PR1 modulator FTY720.

(D) Colonic histologic inflammation scoring for the mice described in (C).

(E) Percent RORγt+ mLN CD4 cells with I-A^b:2W1$S_{55–68}$ specificity in Ca-2W1S colonized mice or I-A^b:CBir1$_{464–472}$ specificity in specific pathogen-free $CD4^{CreER(T2)}$ $KLF2^{f/f}$ mice (red) or Cre-negative littermate controls (black) 20 days after initiating tamoxifen-supplemented chow. Each point indicates the data from an individual mouse, combined from at least two independent experiments each with similar results. *$p < 0.05$, **$p < 0.01$, ****$p < 0.001$, using one-way ANOVA or unpaired t test for two groups; bar, mean ± SEM.

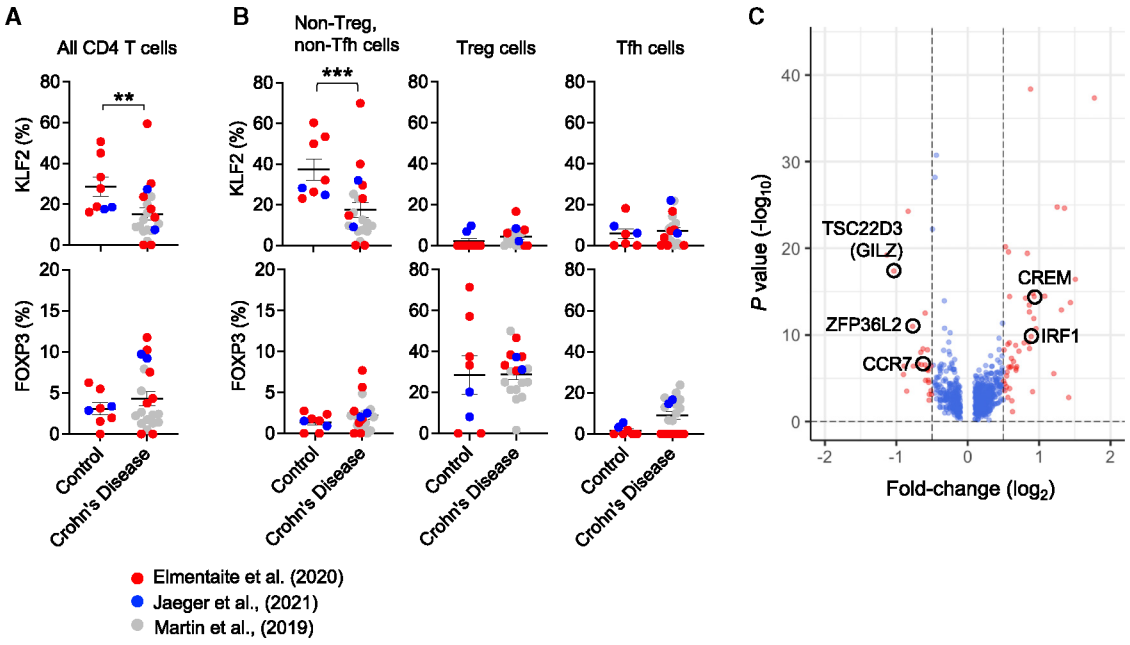

Figure 7. KLF2+ CD4 cells selectively reduced in Crohn's disease

(A) Percent KLF2+ or FOXP3+ among CD4 cells spanning multiple clusters (including Treg and Tfh clusters) in inflamed intestinal biopsy specimens from individuals with Crohn's disease compared with healthy controls pooled from three separate datasets.

(B) Percent KLF2+ or FOXP3+ among cells in individual CD4 cell clusters (non-Treg CD4 cells, non-Tfh CD4 cells, Treg cells, Tfh cells) for the datasets described in (A).

(C) Gene expression comparison for KLF2+ CD4 cells from Crohn's disease compared with controls, showing genes enriched (positive fold change) or repressed (negative fold change) in Crohn's disease. Data from each individual are shown as a single data point color coded by dataset with differences between groups analyzed using the Mann-Whitney U test or one-way ANOVA. **p < 0.01, ***p < 0.005; bar, mean ± SEM. See also Figures S7, S8, and S9 and Tables S3 and S4.

KEY RESOURCES TABLE

REAGENT or RESOURCE	SOURCE	IDENTIFIER
Antibodies		
PE-Cy7 anti-mouse CD4 (clone: GK1.5)	eBioscience	Cat# 25-0041-82; RRID:AB_469576
APC anti-mouse CD4 (clone: GK1.5)	eBioscience	Cat# 17-0041-82; RRID:AB_469320
PE-Cy5 anti-mouse CD4 (clone: GK1.5)	eBioscience	Cat# 15-0041-83; RRID:AB_468696
BV650 anti-mouse CD8 (clone: 53-6.7)	Biolegend	Cat# 100742; RRID:AB_2563056
PE-Cy5 anti-mouse CD8 (clone: 53-6.7)	eBioscience	Cat# 15-0081-82; RRID:AB_468706
PE-Cy5 anti-mouse CD11b (clone: M1/70)	Biolegend	Cat# 101210; RRID:AB_312793
PE-Cy5 anti-mouse CD11c (clone: N418)	Biolegend	Cat# 15-0114-82; RRID:AB_468717
PE-Cy5 anti-mouse F4/80 (clone: BM8)	eBioscience	Cat# 15-4801-82; RRID:AB_468798
PE-Cy5 anti-mouse B220 (clone: RA3-6B2)	Biolegend	Cat# 15-0452-83; RRID:AB_468756
Alexa Fluor 700 anti-mouse CD44 (clone: IM7)	Biolegend	Cat# 56-0441-82; RRID:AB_494011
BV421 anti-mouse CD44 (clone: IM7)	Biolegend	Cat# 103039; RRID:AB_10895752
APC anti-mouse CD44 (clone: IM7)	Biolegend	Cat# 103026; RRID:AB_493713
APC-eFluor780 anti-mouse CD45 (clone: 30F11)	invitrogen	Cat# 47-0451-82; RRID:AB_1548781
FITC anti-mouse FOXP3 (clone: FJK-16S)	eBioscience	Cat# 11-5773-82; RRID:AB_465243
PE anti-mouse FOXP3 (clone: FJK-16S)	eBioscience	Cat# 12-5773-82; RRID:AB_465936
AF647 anti-mouse RORgt (clone: Q31-378)	BD bioscience	Cat# 562682; RRID:AB_2687546
PE-Cy7 anti-mouse IL17A (clone: TC 11-18H10.1)	Biolegend	Cat# 506922; RRID:AB_2125010
APC anti-mouse Helios (clone: 22F6)	eBioscience	Cat# 17-9883-42; RRID:AB_2573322
E450 anti-mouse CD304 (clone: 3DS304M)	eBioscience	Cat# 48-3041-82; RRID:AB_2574051
BV605 anti-mouse CD62L (clone: MEL-14)	Biolegend	Cat# 104437; RRID:AB_11125577
PE-Cy5 anti-mouse CD25 (clone: PC61)	Biolegend	Cat# 102010; RRID:AB_312859
PE-cy7 anti-mouse GITR (clone: DTA-1)	eBioscience	Cat# 25-5874-82; RRID:AB_10548516
PE-Cy7 anti-mouse IRF4 (clone: 34E)	eBioscience	Cat# 25-9858-82; RRID:AB_2573558
BV650 anti-mouse CD90.1 (clone: OX-7)	Biolegend	Cat# 202533; RRID:AB_2562254
Alexa Fluor 700 anti-mouse CD90.2 (clone: 30-H12)	Biolegend	Cat# 105320; RRID:AB_493725
PE-Cy7 anti-mouse CXCR5 (clone: L138D7)	Biolegend	Cat# 145516; RRID:AB_2562210
BV421 anti-mouse BCL6 (clone: K112-91)	BD bioscience	Cat# 561525; RRID:AB_10898007
BV421 anti-mouse T-bet (clone: 4B10)	Biolegend	Cat# 644816; RRID:AB_10959653
E605 anti-moues PD-1 (clone: 29F.1A12)	Biolegend	Cat# 135220; RRID:AB_2562616
BV605 anti-moues Ki67 (clone: 16A8)	Biolegend	Cat# 652413; RRID:AB_2562664
PE-Cy7 anti-mouse CD45.1 (clone: A20)	eBioscience	Cat# 25-0453-82; RRID:AB_469629
PE anti-mouse CD45.2 (clone: 104)	eBioscience	Cat# 12-0454-82 RRID:AB_465678
E450 anti-mouse LAG3 (clone: C9B7W)	eBioscience	Cat# 48-2231-82; RRID:AB_11149866
APC anti-mouse CTLA4 (clone: UC10-4B9)	eBioscience	Cat# 17-1522-82; RRID:AB_2016700
PE-Cy7 anti-mouse CD39 (clone: 24DMS1)	eBioscience	Cat# 25-0391-82; RRID:AB_1210766
Alexa Fluor 700 anti-mouse CD49b (clone: DX5)	eBioscience	Cat# 56-5971-82; RRID:AB_2574507
APC anti-CD226 (clone: 10E5)	Biolegend	Cat# 128810; RRID:AB_2566627
Rat IgG2a (clone: 2A3)	BioXcell	Cat# BE0089; RRID:AB_1107769

REAGENT or RESOURCE	SOURCE	IDENTIFIER
Rat IgG2b (clone: LTF-2)	BioXcell	Cat# BE0090; RRID:AB_1107780
Mouse IgG1 (clone: MOPC-21)	BioXcell	Cat# BE0083; RRID:AB_1107784
Hamster IgG (polyclonal)	BioXcell	Cat# BP0091; RRID:AB_1107773
Rat IgG1 κ (clone: HRPN)	BioXcell	Cat# BE0088; RRID:AB_1107775
anti-mouse CD3 (clone: 145-2C11)	BioXcell	Cat# BP0001-1; RRID:AB_1107634
anti-mouse CD28 (clone: 37.51)	BioXcell	Cat# BE0015-1; RRID:AB_1107624
anti-mouse IL10 (clone: JES5-2A5)	BioXcell	Cat# BE0049; RRID:AB_1107696
anti-mouse IL10R (clone: 1B1.3A)	BioXcell	Cat# BE0050; RRID:AB_1107611
anti-mouse TGFβ (clone: 1D11.16.8)	BioXcell	Cat# BE0057; RRID:AB_1107757
anti-mouse CTLA4 (clone: UC10-4F10-11)	BioXcell	Cat# BE0032; RRID:AB_1107598
anti-mouse LAG3 (clone: C9B7W)	BioXcell	Cat# BE0174; RRID:AB_10949602
anti-mouse OX-40L (clone: RM134L)	BioXcell	Cat# BE0033-1; RRID:AB_1107594
anti-mouse ICOSL (clone: HK5.3)	BioXcell	Cat# BE0028; RRID:AB_1107566
Bacterial and virus strains		
Listeria monocytogenes-2W1S	Ertelt et al.[30]	Derived from WT strain 10403s
Salmonella typhimurium-2W1S	McSorley Lab, University of California, Davis; Benoun et al.[31]	SL1344 ΔAroA
Biological samples		
Candida albicans-2W1S	Kaplan Lab, University of Pittsburg; Igyarto et al.[25]	*CaURA3/CaURA3 pENO1-ENO1-GFP-2W1S-OVA*$_{323-339}$*-OVA*$_{257-264}$*-I-Eα*$_{50-66}$
Chemicals, peptides, and recombinant proteins		
Ampicillin	Sigma-Aldrich	Catalog# A0166
Gentamicin	Sigma-Aldrich	Catalog# G3632
Metronidazole	Sigma-Aldrich	Catalog# M3761
Neomycin	Sigma-Aldrich	Catalog# N6386
Vancomycin	MP Biomedical	Catalog# 0219554005
Sucralose	Sigma-Aldrich	Catalog# 69293-100G
Dehydrated Culture Media: Brain Heart Infusion	Thermo Fisher Scientific	Catalog# B11060
Yeast extract	Boston Bio Product	Catalog# P-950
Bactopeptone BD	Bioscience	Catalog# DF0118170
Uridine	Alfa-Aesar	Catalog# A15227
D-(+)-Glucose	Sigma-Aldrich	Catalog# G5767
Agar	Bio Express	Catalog# J637
DMEM	Gibco	Catalog# 10313-21
Fetal bovine serum	GeneMate	Catalog# S-1200-500
Glutamine (100X)	Gibco	Catalog# 25030-081
HEPES 1M	Gibco	Catalog# 15630-080
Penicillin-streptomycin solution (100X)	Gibco	Catalog# 15140-122
BD Golgi Plug (Brefeldin A solution)	BD Bioscience	Catalog# 555029

REAGENT or RESOURCE	SOURCE	IDENTIFIER
10% normal formalin	Sigma-Aldrich	Catalog# HT501128-4L
Percoll	Sigma	Catalog# P4937
Dnase I	Roche	Catalog# 10104159001
CollagenaseA	Roche	Catalog# 11088793001
DL-Dithiothreitol	Sigma	Catalog# D9779
EDTA	Amresco	Catalog# E177
β-galactosidase peptide		NLSVTLPAASHAIPH
Tamoxifen chow 400 mg/kg	Envigo	Catalog# 130860
CFSE	Thermo Fisher Scientific	Catalog#65-0850-84
Cell stimulation cocktail (500X)	Thermo Fisher Scientific	Catalog#00-4975-03
FTY720	Sigma	Catalog# SML0700-25MG
BrdU	BD Pharmigen	Catalog# 550891
Critical commercial assays		
Mouse Lipocalin-2 Quantikine ELISA	R&D	Catalog# MLCN20
Milliplex (Mouse cytokine/chemokine panel 1)	Sigma-Aldrich	Catalog# MCYTOMAG-70K-PMX
LIVE/DEAD Near-IR staining Kit	ThermoFisher	Catalog# L34976
LIVE/DEAD Blue staining Kit	ThermoFisher	Catalog# L34962
Fixation/Permeabilization solution kit	BD Bioscience	Catalog# 554722
Foxp3/Transcription factor staining buffer set	eBioscience	Catalog# 00-5523-00
Anti-PE Microbeads	Miltenyi	Catalog# 130-048-801
Anti-APC Microbeads	Miltenyi	Catalog# 30-090-855
APC BrdU Kit	BD Pharmingen	Catalog# 552598
SMARTer® Stranded Total RNA-Seq Pico Input Mammalian Kit v3	Takara	Catalog# 634485
Deposited data		
Code for analysis single cell RNAseq and open access human IBD cohort	This paper	https://github.com/Deshmukh-Lab/KLF2_WayLab
Experimental models: Organisms/strains		
CD45.1	Jackson Laboratory	Strain Code: 002014
CD90.1	Jackson Laboratory	Strain Code: 000406
$FOXP3^{RFP}$	Jackson Laboratory	Strain Code: 008374
$CD4^{Cre}$	Jackson Laboratory	Strain Code: 017336
$CD4^{CreER(T2)}$	Jackson Laboratory	Strain Code: 022356
IL10−/−	Jackson Laboratory	Strain Code:002251
Rag1 −/−	Jackson Laboratory	Strain Code:002216
10BiT	Dr. Casey T. Weaver	Maynard et al.[55]
BG-2 TCR	Dr. Dale S. Gregerson	McPherson et al.[51]
$KLF2^{GFP}$	Dr. George Deepe	Lingrel et al.[42]
$KLF2^{f/f}$	Dr. Stephen Jameson	Weinreich et al.[34]

REAGENT or RESOURCE	SOURCE	IDENTIFIER
Software and algorithms		
Prism 6.0h	GraphPad	N/A
Flow Jo 9.9.6	Treestar	N/A
Seurat 4.3.0	Satija Lab	N/A
Sickle 1.33	https://github.com/najoshi/sickle	N/A
Subread	N/A	Liao et al.[82]
DESeq2	N/A	Love et al.[83]
Other		
I-A^b:2W1S_{55-68} Tetramer	NIH Tetramer Core	Moon et al.[27]
I-A^b:CBir1$_{464-472}$ Tetramer	NIH Tetramer Core	Eshleman et al.[84]